Final scientific report for N-INNER:

Synthesis and durability of CNT based MEAs for PEMFC (Nanoduramea)

May 2011

Elina Yli-Rantala
Maryam Borghei
Shuang Ma-Andersen
Sune Veltzé
Alejandro Oyarce
Magnus Thomassen

Project owner

Eva Häkkä-Rönnholm
Vice-President R&D, VTT Technical Research Centre of Finland

Project manager

Pertti Kauranen
Chief Research Scientist, VTT Technical Research Centre of Finland

Project consortium

Dr. Pertti Kauranen - VTT Technical Research Centre of Finland (VTT)
Prof. Esko Kauppinen - Aalto University (Aalto)
Dr. Magnus Thomassen - SINTEF
Prof. Svein Sunde - Norwegian University of Science and Technology (NTNU)
Prof Göran Lindbergh - Royal Institute of Technology (KTH)
Ass.prof. Eivind Skou - University of Southern Denmark (SDU)

Synthesis and durability of CNT based MEAs for PEMFC (Nanoduramea)

Elina Yli-Rantala[1], Antti Pasanen[1], Pertti Kauranen[1], Virginia Ruiz[2], Maryam Borghei[2], Esko Kauppinen[2], Alejandro Oyarce[3], Carina Lagergren[3], Göran Lindbergh[3], Mahdi Darab[4], Svein Sunde[4], Magnus Thomassen[5], Shuang Ma-Andersen[6], Sune Veltzé[6], and Eivind Skou[6]

[1] VTT Technical Research Centre of Finland, P.O. Box 1300, FI-33101 Tampere, Finland
[2] Aalto University, Department of Applied Physics, P.O. Box 15100, FI-00076 Aalto Finland
[3] Royal Institute of Technology, Teknikringen 42, SE-10044 Stockholm, Sweden
[4] Norwegian University of Science and Technology, Sem Sælands vei 12, NO-7495 Trondheim, Norway
[5] SINTEF, Strindveien 4, NO-7465 Trondheim, Norway
[6] University of Southern Denmark, Campusvej 55, DK-5230 Odense, Denmark

Keywords: Carbon Corrosion, Carbon Nanofibers, Carbon Nanotubes, Catalyst Characterization, Catalyst Stability, Catalyst Support, Catalyst Synthesis, MEA degradation, Membrane Electrode Assembly, Proton Exchange Membrane Fuel Cell

Abstract

The objective of the project was to improve the durability of the membrane electrode assemblies (MEAs) of proton exchange membrane fuel cells (PEMFCs) by studying the basic degradation phenomena of carbon supported Pt catalysts and perfluorosulphonated proton conducting membranes. Improved catalysts have been developed by using advanced carbon nanostructures including nanotubes (CNT) and nanofibres (CNF) as the support material and by alloying Pt with base metals, e.g. Co. The surface properties of the carbon nanostructures were modified in order to facilitate for optimum deposition of Pt nanoparticles on these supports as well as to prevent Pt nanoparticle growth on these surfaces.

These advanced catalysts have been characterized with different surface scientific methods, e.g. XRD, SEM, TEM, EDS, ESR and XPS, and dispersed into ionomer inks for MEA fabrication. Laboratory scale MEAs were prepared by drop electrode method or spray coating and have been tested *in situ* in single cell and multisinglecell setups. Standard electrochemical methods such as CV and EIS as well as *in situ* CO_2 monitoring of cathode exhaust gas were used to study the catalyst degradation.

As an outcome, MEA durability improvement by factor of 5 under severe operating conditions was reached.

Executive summary

The main objectives of the project and how they were met is discussed below.

- To increase the stability of the Pt/C catalyst in PEMFC by replacing the conventional carbon black support by carbon nanotubes (CNT), carbon nanofibers (CNF) or novel hybrid carbon nanomaterial, nanobuds (CNB).
    - The catalyst supporting properties of various forms of CNT and CNF materials were evaluated. The use of CNF as support in this project has shown that these support structures lead to enhanced stability towards start/stop cycling of PEM fuel cells at elevated cathode potentials (which may occur e.g. due to fuel starvation).
    - CNB structures could only be synthesized in mg scale and were thus left outside of further studies.

- To increase the durability of the PEMFC MEAs by using optimized Pt (alloy) oxygen reduction catalysts to decrease the concentration of harmful reaction intermediates.
    - As the work on carbon nanostuctures proved scientifically very rewarding only a few experiments were made with Pt alloys.

- To study the interactions between the Pt catalyst and the different carbon nanostructures for optimal deposition of Pt nanoparticles onto the carbon support and preventing the Pt particle growth during FC operation.
    - Different types of carbon supports were examined by various characterization methods, e.g. XPS, Raman, and ESR, to better understand their abilities to function as catalyst support.
    - Activation treatments with acids and polyaniline, as well as by electro-oxidation were employed in order to create binding sites for Pt catalyst nanoparticles on the surface of the support material
    - Several different Pt deposition methods were also employed. Deposition by polyol method proved to be optimal in terms of achieved Pt loading, Pt particle size, and particle distribution.

- To develop analytical tools to study the membrane and catalyst ageing phenomena.
    - A method to study accelerated ageing of the catalyst was developed.
    - Online monitoring of the exhaust gas using FTIR from laboratory PEM fuel cells was established. Using this analytical tool it was possible to investigate carbon degradation from the catalyst support through the detection of CO and CO_2. It was also possible to detect membrane degradation by monitoring the emission of HF (especially during dry operation).
    - CO stripping as a tool for investigating the particle size and degree of agglomeration of Pt nanoparticles on carbon structures was developed during the project.
    - The use of an electrochemical quartz crystal microbalance for real time determination of Pt dissolution and particle growth from Pt/C electrocatalysts was also developed.
    - Post mortem investigation of MEAs by SEM and EDX was developed.
    - A multisinglecell setup was developed for face to face comparison to different catalysts and their degradation rates.

- To improve the quality and reproducibility of the MEA preparation techniques for reliable *in situ* FC testing of the nanotube based catalysts.
    - The reproducibility was studied in the multisinglecell setup.

- Education of FC scientists by organization of annual PhD summer schools within the research field.
    - Qualified personnel were trained by networking and sharing competence and knowledge with other participants.
    - The first summer school was organized in Espoo, Finland, in summer 2008. The summer school was titled "Synthesis and characterization of carbon nanotubes and nanofibers".
    - Another successful PhD summer school was arranged in Trondheim, Norway, in summer 2009 with about 50 participants. Internationally renowned speakers from Europe and North America held lectures on the theme "Synthesis and characterization of carbon supported platinum and platinum alloy catalysts".

- Similarly, a summer school entitled "The membrane electrode assembly (MEA) in PEMFC" was arranged in summer 2010 in Utö, Sweden, with five internationally recognized speakers. Presentations by the PhD students working within the project were heard as well.
- Public presentations were published via project web pages on the internet.

Several methods related to catalyst support functionalization, catalyst synthesis, material characterization and electrochemical evaluation were used.

- Support functionalization
  - Acid treatment with varying acid concentration, refluxing time, and temperature
  - Electro-oxidation
  - Polyaniline treatment
- Catalyst synthesis
  - Impregnation method
  - Organometallic synthesis
  - Polyol method
  - Modified polyol method
- Material characterization and electrochemical evaluation
  - FTIR, ESR, XPS, Raman for characterization of the catalyst support surface
  - RRDE for quantization of peroxide formation
  - TGA, XRD, SEM and TEM for examining the Pt loading, particle size and particle distribution after the Pt deposition
  - TGA for carbon thermal corrosion and decomposition in Pt catalysts
  - CO stripping and CV for catalyst active area determination
  - Polarization curves in real fuel cell conditions for evaluating the fuel cell performance
  - EQCM for determining the Pt dissolution rate upon chloride exposure
  - CV studies in single cell combined with AAS for determining Pt dissolution as a function of applied potential
  - High voltage cyclic treatment in single cell for electrochemical stability studies
  - Single cell and multisinglecell mounted with different MEA combinations for fuel cell performance studies
  - PEM fuel cell test station connected to FTIR gas spectrometer analyzing cathode exhaust gas for carbon degradation studies

Of the results concerning the catalyst support functionalization, the acid treatment of graphitized carbon nanofibers with diluted acids was not capable of forming significant amount of oxygen functionalities on the very stable fiber surface. In addition, the amount of polyaniline used in the polyaniline treatment of carbon nanofibers was too high, as the traces of polyaniline harmed the long-term electrochemical activity of the catalyst.

Of the results concerning the work done with catalyst synthesis, the polyol method showed the best results regarding better dispersion of Pt nanoparticles with more controlled and smaller particle size. Morphological characterizations combined with analytical RRDE measurements and subsequent corrosion/stability tests in fuel cell environment confirmed that highly graphitized carbon nanofibers showed the highest stability and durability in the fuel cell.

It was also shown that the determination of the electroactive surface area is of high importance when it comes to understand the degradation of catalyst and its support. For that CO stripping is a more reliable method than to study the peaks for underpotential deposition of hydrogen. In studies concerning the durability of the supported catalyst, the method of accelerated degradation is very important in order to mimic conditions in real fuel cell. In addition, it was shown that the type of carbon support has a large influence on both carbon corrosion and platinum catalyst stability.

The obtained results have been communicated at several international conferences and in scientific publications for the benefit of the whole fuel cell community. Furthermore, IRD A/S was responsible for the MEA fabrication and therefore benefited from the experience it gained during the fabrication process.

The results from this project showed that there is a significant room for improvement of the carbon materials used as supports for PEM fuel cell catalysts when it comes to the stability towards carbon corrosion induced

under real use of these PEM fuel cells. More specifically, further efforts should be done to e.g. modify the surface of the support by doping or trying some new methods to deposit Pt in order to increase the chemically active surface area of the catalyst and to achieve higher initial activity in the fuel cell while achieving good long-term stability. It could also be advantageous to fully examine the catalyst supporting potential of carbon nanofibers with different structures.

It would be especially important to extent the scope of the studies to high-temperature PEMFC in which the corrosion phenomena are accelerated and to non-carbon catalyst supports, e.g. semiconducting oxide type of supports.

All in all, there is clearly a need for further research and materials development within this field in order to increase the durability and reduce the costs of this technology. The results have direct implications to catalyst producers and also PEM fuel cell stack manufacturers who can target increased durability in their materials development.

These types of Nordic collaborative projects are very good in order to create synergies of the cooperation of Nordic research institutions and industry with various unique competences. These projects also facilitate the spread of leading international knowledge between the Nordic partners and to the next generation of Nordic scientists within the field. It is highly recommended that these types of projects continue to be funded.

Internationally, it is a clear strategy in funding research and technology development of hydrogen and fuel cell technologies. The European Union, Germany, US, Canada and Japan all have large research programs within this field with large industry participation. It is highly recommended that the Nordic countries again focus on this research field in their calls.

1 Catalyst support synthesis

1.1 Support materials used in the project

Most of the materials used for the catalyst supporting purposes were commercial grade carbon nanotubes (CNTs), carbon nanofibers (CNFs) and carbon black (CB), of which the latter was used as a reference material. Of the CNTs, in addition to single-wall carbon nanotubes (SWCNTs), also few-wall carbon nanotubes (FWCNTs), and multi-wall carbon nanotubes (MWCNTs) were used. Some carbon materials were available in graphitized form, which means that the material has been heat-treated in very high temperatures giving the material a highly ordered structure and very good stability. When a graphitized form is wanted to distinguish from the ungraphitized form, a letter "G" is added in front of the abbreviation; e.g. GMWCNTs. Only types of supports that were actually synthesized within the project were some of the used SWCNTs and FWCNTs. The synthesis of these carbon nanomaterials was conducted at Aalto University.

Table 1.1 summarizes the types of carbon nanomaterials used for catalyst supporting. As the aim of the project was to find alternatives to commonly used carbon black catalyst support, the table lists only the alternative materials and states Vulcan as the reference material. The characteristics of various other types of carbon blacks were examined within the project as well, but due to their great number, only the mainly used Vulcan is included in the table.

Table 1.1. Abbreviations and information of the carbon materials used for catalyst supporting.

Used abbreviation	Trade name	Supplier	Support type
SWCNT	-	Aalto University	single-wall CNT
FWCNT	-	Aalto University	few-wall CNT
GMWCNT	Timestub™ TNGM2	Timesnano	graphitized multi-wall CNT
GNF (SD-CNF)	VGCF™	ShowaDenko K.K.	graph. carbon nanofiber (150 nm)
VGF	VGCF-X™	ShowaDenko K.K.	carbon nanofiber (15 nm)
Vulcan*	Vulcan XC-72	BASF	carbon black

* Used as a reference catalyst support.

GNFs are highly graphitized carbon nanofibers with an approximate diameter of 150 nm and a length of 10 μm. VGFs are smaller, with a diameter of about 15 nm and length of 3 μm.

1.2 FWCNT and SWCNT synthesis

FWCNTs were synthesized by decomposition of methane on MgO supported Co-Mo catalyst. The catalytic pyrolysis was carried out by CH_4 diluted with 80 % H_2 at 950º C according to the method reported by the group[1]. FWCNTs with 2-5 walls, around 6 nm diameter and 1 μm length were obtained by this chemical vapor deposition (CVD) method. Figure 1.1 shows the schematic of the reactor and TEM mage of the FWCNTs produced.

[1] Yu.V. Gavrilov, D.A. Grishin, H. Jiang, N.G. Digurov, A.G. Nasibulin, E.I. Kauppinen, Russian Journal of Physical Chemistry A, 2007, Vol. 81, No. 9, pp. 1502–1506.

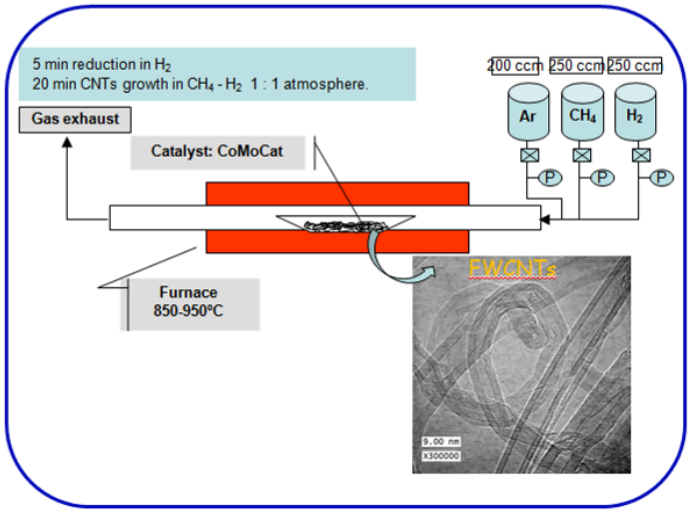

Figure 1.1. Experimental set-up for FWCNT CVD synthesis and TEM image of the product.

SWCNTs were produced by floating catalyst CVD using CO as carbon source and ferrocene as catalyst precursor. After the synthesis, metal residuals originating from the catalyst were purified by washing the product with HCl, followed by rinsing with deionized water and drying in vacuum. Finally, the metal residue content after purification procedure was estimated by thermogravimetric analysis (TGA). The typical values obtained were less than 0.5 wt%.

2 Catalyst support functionalization

Graphitized carbon nanofibers, as the GNFs used in this project, are very inert and durable even in oxidative environment such as the cathode of a fuel cell. The graphitic nature of GNFs is however also a drawback: the catalyst nanoparticles do not easily find anchoring sites on the surface of the fibers. Due to this, it was considered to be advantageous to create binding sites, i.e. different functional groups, on the surface of the fibers.

2.1 Acid treatments

One means for functionalization was subjecting the fibers to oxidative treatment by acids. Different intensities were trialed by changing the nature of the acids (HNO_3, H_2SO_4, or mixture of them), refluxing time and temperature, to optimize the treatment to achieve the maximum number of anchoring sites with minimum damage to the GNFs. FWCNTs were functionalized by the same manner as GNFs. Table 2.1 presents the summary of the acid treatments performed for GNFs at VTT. Similarly, Table 2.2 summarizes the parameters used in the oxidation of the FWCNTs at Aalto University.

Table 2.1. Acid treatment parameters used in the oxidation of the GNFs.

Sample	Acid	Concentration (M)	Time (h)	Temp (°C)
GNF-001	H_2SO_4	concentrated	2	90
GNF-002	H_2SO_4	4	2	90
GNF-003	HNO_3	2	2	90
GNF-004	H_2SO_4/HNO_3	4/2	2	90
GNF-005	H_2SO_4	4	8	120
GNF-006	HNO_3	2	8	120
GNF-007	H_2SO_4/HNO_3	4/2	8	120

Table 2.2. Acid treatment parameters used in the oxidation of the FWCNTs.

Sample	Acid	Concentration (M)	Time (h)	Temp (°C)
FWCNT_1	Just catalyst removal (HCl washing)			
FWCNT_2*	H_2SO_4/HNO_3	1/2	2	120
FWCNT_3*	H_2SO_4/HNO_3	1/2	4	120
FWCNT_4	H_2SO_4/HNO_3	1/2	6	120

*) Catalyst removal by HCl washing after the FWCNT synthesis included.

2.2 Electrochemical oxidation

In addition to chemical oxidation by acids, also electrochemical oxidation of various types of carbon materials was conducted. An overview of the carbon samples treated electrochemically at SDU is provided in Table 2.3.

Table 2.3. Overview of electrochemically treated carbon support materials.

Sample name	Carbon type	Treatment conditions
SD-OxHi	CNF (GNF)	Electrochemical[a], 7000 cycles, Quinone[b]
SD-OxLo	CNF (GNF)	Electrochemical[a], 6700 cycles, Hydroquinone[c]
V-OxHi	CB (Vulcan)	Electrochemical[a], 6500 cycles, Quinone[b]
V-OxLo	CB (Vulcan)	Electrochemical[a], 7000 cycles, Hydroquinone[c]
A-OxHi	Acetylene black	Electrochemical[a], 9200 cycles, Quinone[b]
A-OxLo	Acetylene black	Electrochemical[a], 8000 cycles, Hydroquinone[c]

[a)] Electrochemically oxidized by sweeping between 0.04-1.3 vs. DHE at 100 mV/s. [b)] Electrochemical cycling stopped at potential higher than 0.8 V vs. DHE. [c)] Electrochemical cycling stopped at potential below 0.6 V vs. DHE.

Acetylene black is a type of carbon black produced by Hydrocell Ltd.

2.3 Polyaniline treatment

Similar to functional groups containing oxygen, also nitrogen functionalities on the support surface can act as anchoring sites for platinum nanoparticles[2]. The method for nitrogen functionalization used in the project was by synthesizing a GNF-polyaniline composite, followed by pyrolyzing the composite in nitrogen atmosphere. The objective of the pyrolysis was to decompose polyaniline (PANI), which is aromatic polymer containing nitrogen in its backbone, and leave only small nitrogen functionalities on the fiber surface.

PANI treatment was chosen because the source material, carbon nanofiber-polyaniline composite, was readily provided by another research team at VTT. Two types of samples were received with varying PANI content: one containing a threefold amount of PANI in comparison to the mass of GNFs, and another containing a tenfold amount of PANI. These sample types were identified as SD+3xPANI and SD+10xPANI, respectively, where SD refers to ShowaDenko, the supplier of the GNFs.

The received composite material was purified by washing with ammonia, ethanol and water. After washing, the product was dried in vacuum overnight. The appropriate pyrolysis temperature was resolved by thermogravimetric analysis (TGA) and Fourier transform infrared spectroscopy (FTIR) as follows. Both sample types, SD+3xPANI and SD+10xPANI, were heat treated for 20 min under nitrogen gas flow in different temperatures (300, 600, 700, 800, and 900 °C) while observing the consequent mass loss by TGA. The results were similar in both cases; the achieved percentage of pyrolyzed PANI increased intensively when going from 300 °C to 600 °C after which it grew more steadily, and hardly any difference was observed between treatments in 800 °C and 900 °C. This behavior is illustrated by the graph in Figure 2.1.

[2] A. Hirsch, *Angewandte Chemie International Edition* 2002, 41, 1853.

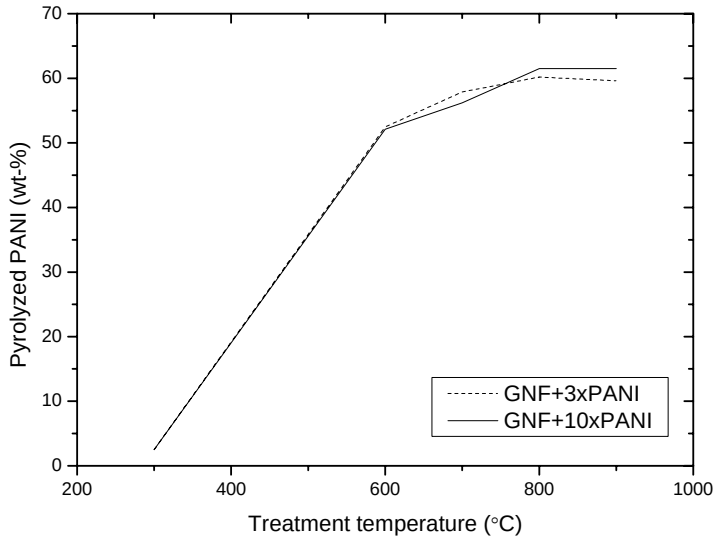

Figure 2.1. Proportion of pyrolyzed PANI as a function of the treatment temperature.

The FTIR analysis supported the TGA results. Figure 2.2 shows the FTIR spectra of SD+3xPANI samples. The characteristic peaks of polyaniline are visible in the spectra of untreated samples as well as in samples treated in 300 °C, although in the latter case the peaks have slightly been shifted indicating that some chemical changes had already occurred.

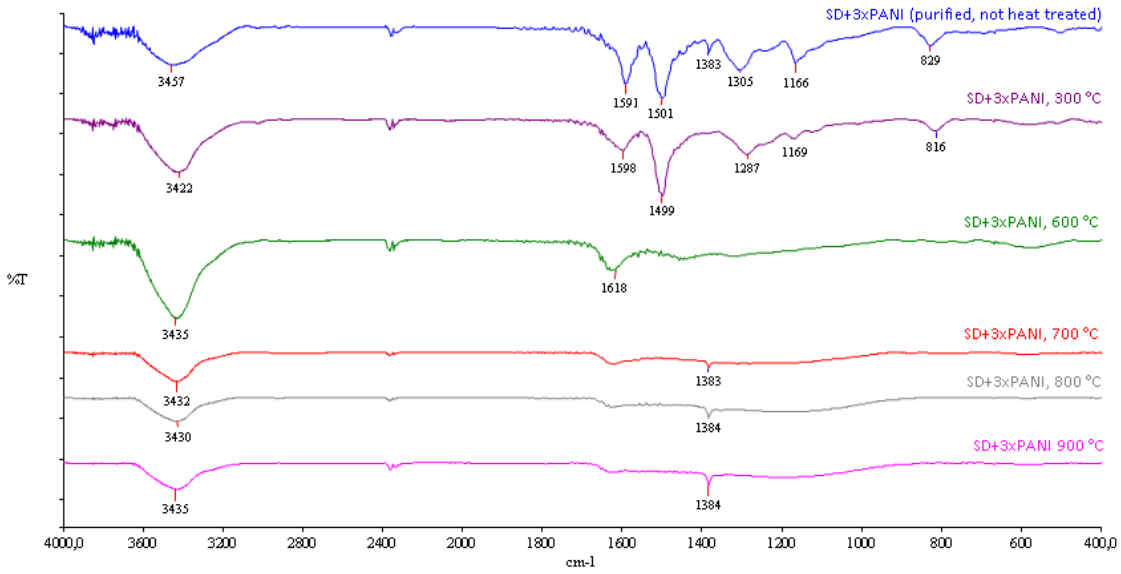

Figure 2.2. FTIR spectra of SD+3xPANI samples heat treated in nitrogen atmosphere in different temperatures. The spectrum of the purified but not heat treated material is presented as a reference.

In samples treated in 600 °C the absorption bands were already clearly changed, and the bending vibration of *p*-disubstituted benzene ring at 829/816 cm^{-1} had disappeared. The samples treated in higher temperatures, 700 °C, 800 °C, and 900 °C, showed only one characteristic peak, 1 384 cm^{-1}, in addition to the OH stretching vibration around 3 430 cm^{-1} present in all samples. The signal at 1 384 cm^{-1} was assumed to be due to C–N stretching vibration in the neighborhood of a quinonoid ring[3], which indicated that the objective of forming C-N bonding on the fiber surface had been realized.

[3] Trchová, M., Konyushenko, E.N., Stejskal, J., Kovářová, J., et al. 2009. Polymer Degradation and Stability 94, 6, pp. 929-938.

2.4 Commercial functionalized materials

Some materials were acquired ready-functionalized. These materials consisted of OH and COOH functionalized graphitized MWCNTs, which are presented by Table 2.4.

Table 2.4. Commercially available functionalized GMWCNTs used in the project.

Sample	Amount of functionality (wt%)	Trade name	Manufacturer
GMWCNT-OH	1.85	Timestub™ TNGMH2	Timesnano
GMWCNT-COOH	1.20	Timestub™ TNGMC2	Timesnano

3 Catalyst support characterization

Various techniques were employed in order to examine the characteristics of different types of (unfunctionalized or functionalized) carbon support alternatives.

3.1 FTIR

Acid treated GNFs were first characterized by Fourier transform infrared spectroscopy (FTIR) at VTT. The used hardware was Perkin Elmer Spectrum BX FT-IR system, and the analyses were performed by using KBr pellet technique. The spectra were recorded in the 400 - 4 000 cm^{-1} wave number range. The high absorbability of carbonaceous nanomaterials in the IR spectral range is well recognized problem that causes the transmittance to be very low[4]. Due to this, the intensities of the characteristic peaks in the spectra were very low, which made the interpretation of the peaks difficult. Figure 3.1 shows as an example a set of FTIR spectra obtained.

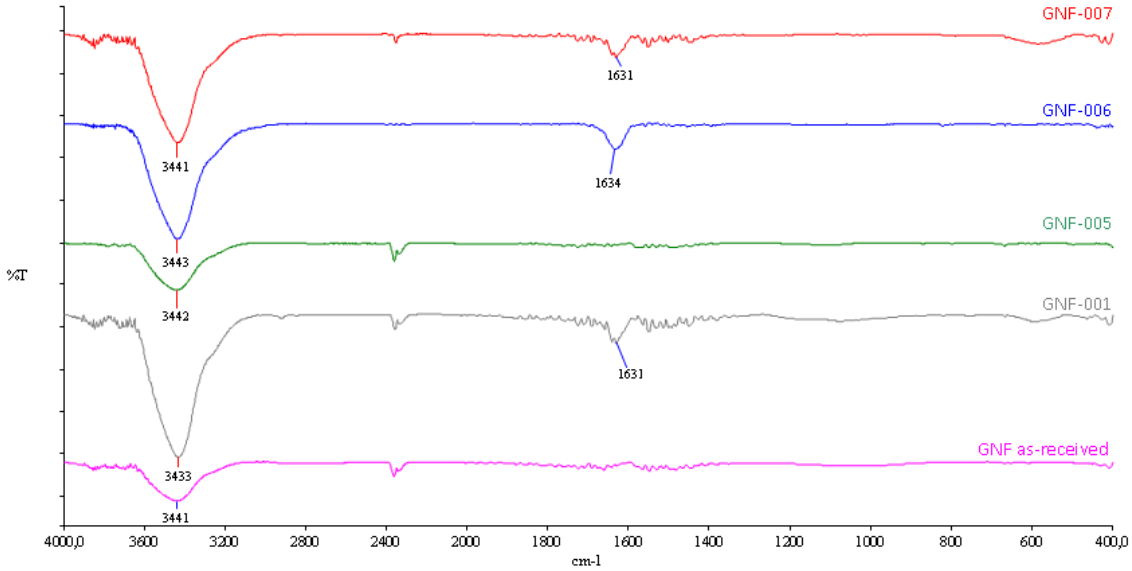

Figure 3.1. FTIR spectra of oxidized samples acid treated for 8 hours at 120 °C. Untreated GNF is shown as a reference sample.

Only OH type oxygen functionalities were found, as can be seen by the absorption band at approximately 3440 cm^{-1}. The signal may however be partly or mostly due to the water vapor in air. On the basis of the FTIR results it can be said that it is probable that the acid treatments used were too mild for the very durable GNFs and did not cause a significant increase in the extent of surface oxidation.

3.2 XPS

An X-ray photoelectron spectroscopy (XPS) measurement is a quantitative method for revealing the relative ratio between specific surface species. X-ray photoelectron spectroscopy measurements were made in collaboration with Per Morgen from the Institute of Physics and Chemistry at SDU in Odense.

The untreated and acid treated carbon samples were prepared by spreading a few milligrams of the carbon powder on an approximately 1 cm^2 large piece of adhesive aluminum tape by the use of a cotton Q-tip. The electrochemically treated carbon samples were transferred to the adhesive aluminum tape after electrochemical treatment on a piece of gold sheet. The pieces of aluminum tape were mounted on a sample holder by double adhesive electronically conductive carbon tape and introduced into the vacuum chamber.

[4] J. Zhou, Z. Sui, J. Zhu, P. Li, D. Chen, Y. Dai, W. Yuan, *Carbon* **2007,** 45, 785.

All XPS analyses were conducted in ultrahigh vacuum (10^{-10}-10^{-8} mbar). The X-ray source was a magnesium anode emitting Mg K_α photons with the energy of 1253.6 eV. The XPS spectrometer was a home built system, largely made up of SPECS components. Overview spectra in the range 0-860 eV were measured from the samples with the step size of 0.5 eV and the pass energy of 80 eV. Detailed scans C 1s of the binding energies in the range 260-360 eV were composed of 5 scans with steps of 0.1 eV and a pass energy of 40 eV. Similarly the spectra at the O 1s binding energies were recorded by 5 scans at 520-590 eV, 0.1 eV steps, and 40 eV pass energy. The count time was 0.5 s, the applied X-ray power was 125 W, and the detector and bias voltages were 2600 V and 90 V, respectively, for all measurements.

Data processing was performed by the use of the software CasaXPS. The peak representing the C 1s electrons was allotted the value 284.6 eV and used as a reference. Integration in the peak regions was performed using Shirley backgrounds. The atomic compositions of the samples were calculated from the areas of the signals in the overview spectrum by the use of appropriate instrument-specific sensitivity factors.

From the overview spectra, see Figure 3.2, the integrated C 1s and O 1s signals revealed the relative surface composition. Deconvolution analysis of each signal gave more detailed compositional information.

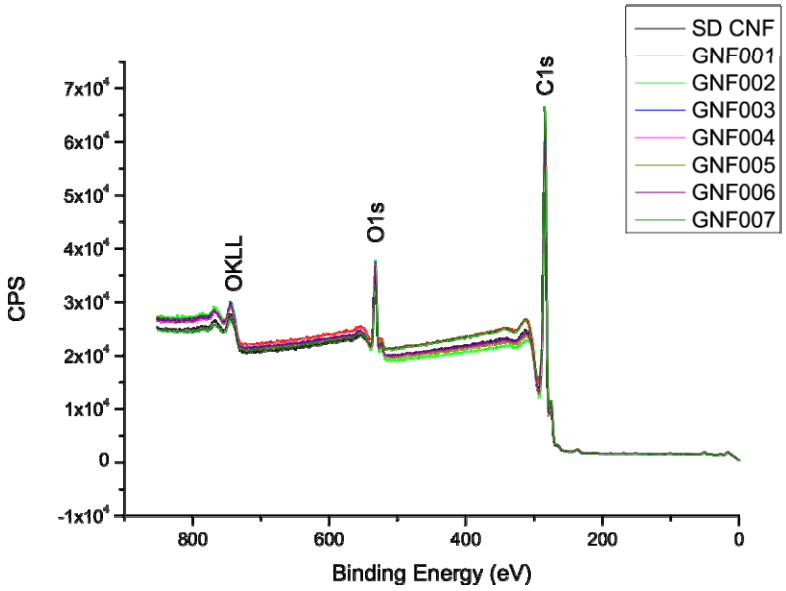

Figure 3.2 XPS overview spectra of the acid treated GNF samples having untreated GNF (SD CNF) as a reference.

The deconvolution of the specific C 1s XPS signal was made by fitting to pure Gaussian peaks on a Shirley background. The deconvolution of the acid treated samples proved tedious, as the signals were not well resolved. The wide signals meant that a conservative approach to quantify the signal species had to be employed. As the overview composition of oxygen to carbon was needed to be the same in the deconvoluted signals, restraints were put to deconvolution peaks. The restraints consisted of area constraints, in which none of the oxygen containing species areas was allowed to be more than 10 % of the carbon signal, and restraints to the peaks. Despite these restraints, the deconvolution was somewhat imprecise, as the area of the C-O, C-OH and C=O peaks usually reached its highest limit. However, from the atomic composition some effect of the acid treatment on the surface structural composition could be made. The compositional information for the acid treated samples is shown Table 3.1.

Table 3.1. XPS compositional data of acid treated and electrochemically oxidized samples. Carbon and oxygen compositional data from overview spectra and detailed compositional assessment from C 1s peak.

Sample name	Atomic C (%)	Atomic O (%)	-COOH (%)*	-C=O (%)*	-C-O, -C-OH (%)*
GNF	94.6	5.4	13.6	8.2	8.2
GNF-001	93.9	6.1	15.2	7.2	7.3
GNF-002	91.0	9.1	7.8	7.2	7.2
GNF-003	92.1	7.9	7.5	7.0	7.0
GNF-004	92.3	7.7	7.6	7.0	7.0
GNF-005	92.1	8.0	7.6	7.0	7.0
GNF-006	90.8	9.2	7.4	6.9	6.9
GNF-007	95.1	5.0	7.2	6.7	6.7
SD-OxHi	90.8	8.5	12.7	22.8	12.0
SD-OxLo	93.1	5.9	9.3	12.1	26.4
V-OxHi	84.9	15.1	0	9.3	0
V-OxLo	87.8	12.2	0	21.1	3.4
A-OxHi	91.3	8.7	0	15.8	19.6
A-OxLo	91.4	8.6	0	13.7	13.5

* Percentage from the amount of carbon.

In general, the oxygen content seemed slightly elevated compared to the untreated fibers. The fibers, which had underwent the harshest acid treatment (4 M H_2SO_4 and 2 M HNO_3 at 120 °C) seemed to have less oxygen content after treatment than before treatment. The acid treatment with 4 M H_2SO_4 at 90 °C or 2 M HNO_3 at 120 °C seemed to yield the same oxygen content (GNF-002 and GNF-006, respectively).

Table 3.2 presents the surface compositions determined by the XPS from the overview spectra.

Table 3.2. Surface compositions of Vulcan, acid treated FWCNT samples, one untreated and two functionalized GMWCNT samples, and untreated GNFs determined by XPS.

Sample	Carbon concentration (at%)	Oxygen concentration (at%)	Fluorine concentration (at%)
Vulcan	97.3	2.7	–
FWCNT_1	98.5	1.5	–
FWCNT_2	98.1	1.9	–
FWCNT_3	98.2	1.8	–
FWCNT_4	98.9	1.1	–
GMWCNT	98.4	1.1	0.5
GMWCNT-OH	95.1	3.9	1.0
GMWCNT-COOH	97.6	1.8	0.7
GNF	98.2	1.1	0.7

The FWCNT_2 and FWCNT_3 which were purified and boiled in oxidizing acid had a little higher oxygen content than only-purified FWCNT. However, the treatment time (2 h for FWCNT_2 and 4 h for FWCNT_3) did not seem to affect the oxygen concentration. The one-step-treated (6 h) FWCNT_4 contained less oxygen than the other samples, which indicated that the HCl purification step was important for the introduction of oxygen functionalities.

For the GMWCNTs, higher oxygen contents were found in the hydroxyl- and carboxyl-functionalized samples, GMWCNT-OH and GMWCNT-COOH, respectively. In both cases the obtained oxygen concentrations were higher than the contents stated by the manufacturer, which were 1.85 wt% OH corresponding to 1.3 at% O and 1.20 wt% COOH corresponding to 0.64 at% O, respectively. These divergences were maybe due to the presence of other oxygen-containing species or differences between surface and bulk compositions.

As a conclusion of the XPS analysis technique, the measurements made on the acid treated fibers and a variety of electrochemically treated samples revealed that the specific species quantization is possible. However, as the quantization consists of mathematical fitting on physical responses, some degree of error may occur. Furthermore, specific restraints must be imposed on the fitting functions, as specific species composition can not exceed overall atomic composition.

3.3 ESR

Samples for electron spin resonance spectroscopy (ESR) analysis were prepared by mixing the carbon material with MgO. ESR spectra in a 400-G magnetic range comprising the appearing signals about a *g* value of 2.0 were recorded at room temperature with a BRUKER EMP-A/A/P system at SDU. Microwave radiation with a fixed frequency in the range of 9.42-9.86 GHz was used. Data was acquired as first derivatives of absorption, and 10 scans recorded with a step size of 0.4 or 0.5 G were accumulated for each spectrum. The software used for control, data acquisition, and spectral analysis was BRUKER Xenon 1.1 b.22.

The intensity of the carbon signal was corrected for the total contribution from the MgO, which was calculated from the intensity of the MgO reference peak in the spectrum in question. The corrected carbon intensity was then divided by the intensity of the reference peak to yield the relative signal intensity.

The carbon signal looked somewhat as a singlet, however it was broad and asymmetric. When looking closer at the carbon singlet, see Figure 3.3, it became even more apparent. The carbon signal was probably a collection of signals, which indicated that there were multiple spin active species present.

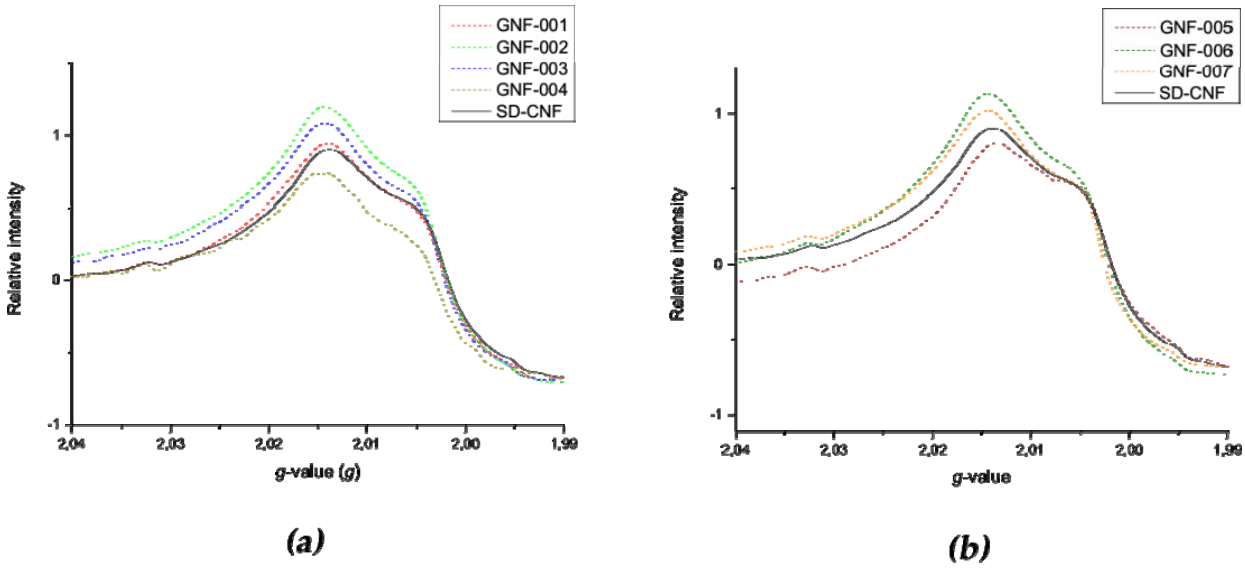

Figure 3.3. ESR spectra of acid treated carbon samples at (a) 90 °C for 2 h and (b) at 120 °C for 8 h compared to the untreated GNF sample (SD-CNF).

The investigations revealed that the acid treatment at lower temperature (90 °C) made almost none or only little change to the signal due to localized electrons in the defect states. On the contrary, the acid treatment seemed to raise both conduction electron signal and localized defect site electron signals. For the higher-temperature acid treated GNF samples, both decrease in conduction electron signal or increase in conduction electron signal was found, GNF-005 and GNF-007, respectively, depending on the acid composition.

FWCNTs showed a relatively high concentration of defects in addition to the expected abundance of conduction electrons. Otherwise the ESR results for the samples of this material were somewhat inconclusive. However, when combined with the oxygen contents determined by XPS, it could be proposed that purification in HCl prior to acidic oxidation was important for the generation of structural changes.

3.4 Raman spectroscopy

Raman spectra were recorded on a Bruker Ramanscope III combined Fourier transform and dispersive Raman spectroscopy instrument at SDU. The spectra were recorded in the 1800-500 cm^{-1} region and the intensities were calculated by using OPUS 6.5sp1 software.

The overview Raman spectra of the different untreated carbon substrates can be seen in Figure 3.4.

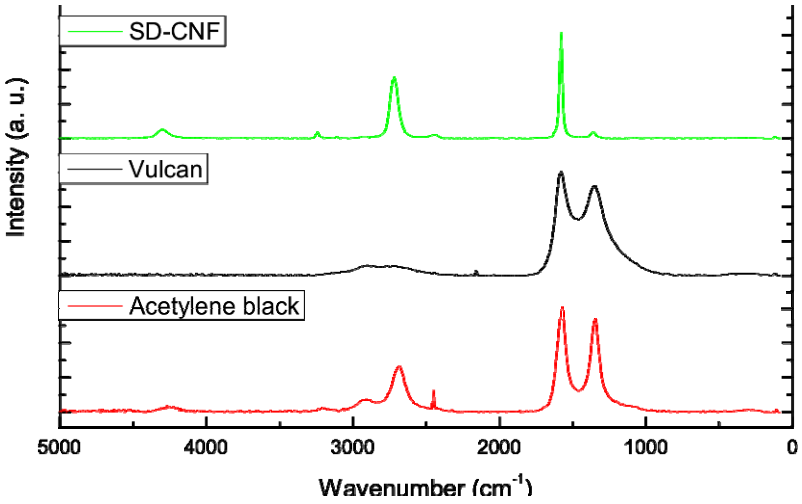

Figure 3.4. Overview Raman spectra of GNFs (SD-CNF), Vulcan, and Acetylene black.

The Raman spectra of the different carbon samples appeared very different. The Acetylene black samples exhibited Raman spectrum with vibrational bands occurring from 1000-4500 cm^{-1}. The Vulcan sample exhibited strong D and G-band vibrations only, whereas the GNF sample had a low intensity D-band vibration, implying a high degree of graphitization.

The acid treated samples were measured without any prior treatment: the samples were placed on a piece of aluminum coated glass. The electrochemically oxidized samples were placed on a piece of adhesive aluminum tape, from which the measurement was made. The aluminum supports reflectively enhanced the Raman signal.

The quantification of defect sites was made by normalizing the D and G'-band intensities with the G-band intensity of the relevant spectrum. The quantification of the amount of defects using the I_D/I_G ratio exhibited a somewhat unexpected result. The ratio of I_D/I_G was exceptionally low for all GNF samples, consistent with a high degree of graphitization. However, the degree of change exhibited by the acid treated fibers was very low. The electrochemically treated fibers exhibited a higher degree of change. For the remaining samples, the I_D/I_G ratio seemed to decrease when the carbon samples were subjected to electrochemical treatment, which implies that the defect sites (or amorphous carbon) had been converted into graphitic structured carbon or removed. This was expected for the carbon black samples, as they generally contain more defect sites than structured carbon nanotubes.

The $I_{G'}/I_G$ ratio seemed to follow the expected trend, as the ratio increased for all acid treated GNF samples except GNF-002 and GNF-003. These samples seemed to contain fewer defects, which were also seen by the ESR measurements. The electrochemically treated Acetylene black samples exhibited lower $I_{G'}/I_G$ ratios, which could be expected as the electrochemical treatment would restructure the carbon surface. The highest $I_{G'}/I_G$ ratio for the acid treated samples was achieved by GNF-006, which also seemed from ESR measurements to contain the most defect sites.

3.5 Peroxide formation from the carbon ORR

The kinetics of the oxygen reduction reaction (ORR) for the untreated and acid treated carbon samples were measured by a rotating ring disk electrode (RRDE). By using the relationship in Eq. 3.1, the peroxide formation

was quantized for these samples and a relationship of the peroxide formed at the anodic electrode materials could be seen. *N* is the collection efficiency of the RRDE, which must be determined experimentally.

$$X_{H_2O_2} = \frac{\frac{2I_R}{N}}{-I_D + \frac{I_R}{N}} \qquad \text{(Eq. 3.1)}$$

The determined peroxide formation percentages can be seen in Figure 3.5. The peroxide is formed at low oxidation potentials. The percentage peroxide formation is shown for the 0-200 mV oxidation potential, as this is the area where the peroxides are formed at the carbon substrates. Above 200 mV the signal is very affected by noise.

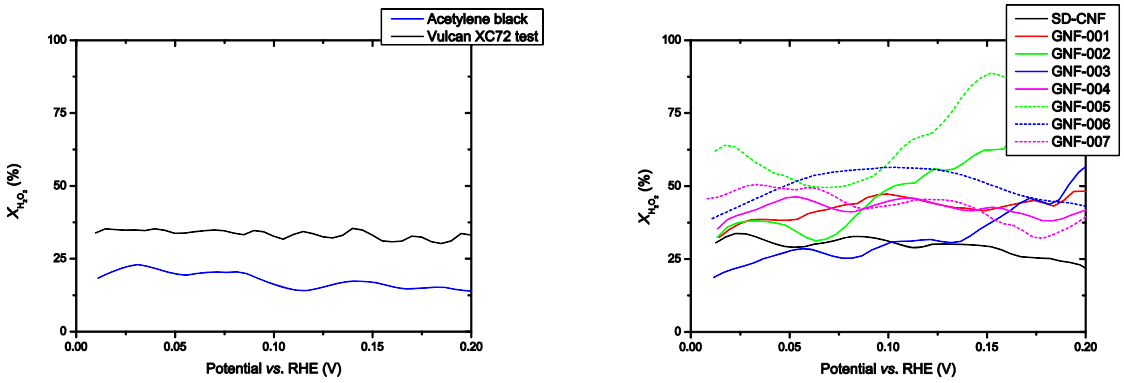

Figure 3.5. Percentages of peroxide formed in the range 0-200 mV vs. RHE on thin-film electrodes of Vulcan and Acetylene black (left), and the untreated and acid treated GNFs (right). The percentage of peroxide formation of the GNFs acid treated at 120 °C (GNF-005 to GNF-007) are drawn by dashed lines.

By the carbon black substrates in Figure 3.5 (left) can be seen that the formed peroxide levels were steady at approximately 30 % for Vulcan and 20 % for the Acetylene black samples. The lower peroxide formation for the Acetylene black was due to its higher degree of orientation, whereas Vulcan is more amorphous carbon.

For the untreated GNF, the measured peroxide formation was almost just as high as for Vulcan (30 %). When examining the effect of acid treatment on the peroxide formation, a slight increase in percentage peroxide formation could be noted. Although, the nitric acid treated GNF-003 exhibited a lower percentage peroxide formation near 0 V than the untreated fibers.

The effect of higher-temperature acid treatment on the formation of peroxide was drastic, as the sulphuric acid treated fibers GNF-005 (120 °C), seemed to generate almost double the amount of peroxide than the fibers treated at 90°C (GNF-002). This undoubtedly was an effect due to the added oxygen containing defect sites.

Figure 3.6 shows the peroxide formation in the case of other oxygen functionalized materials.

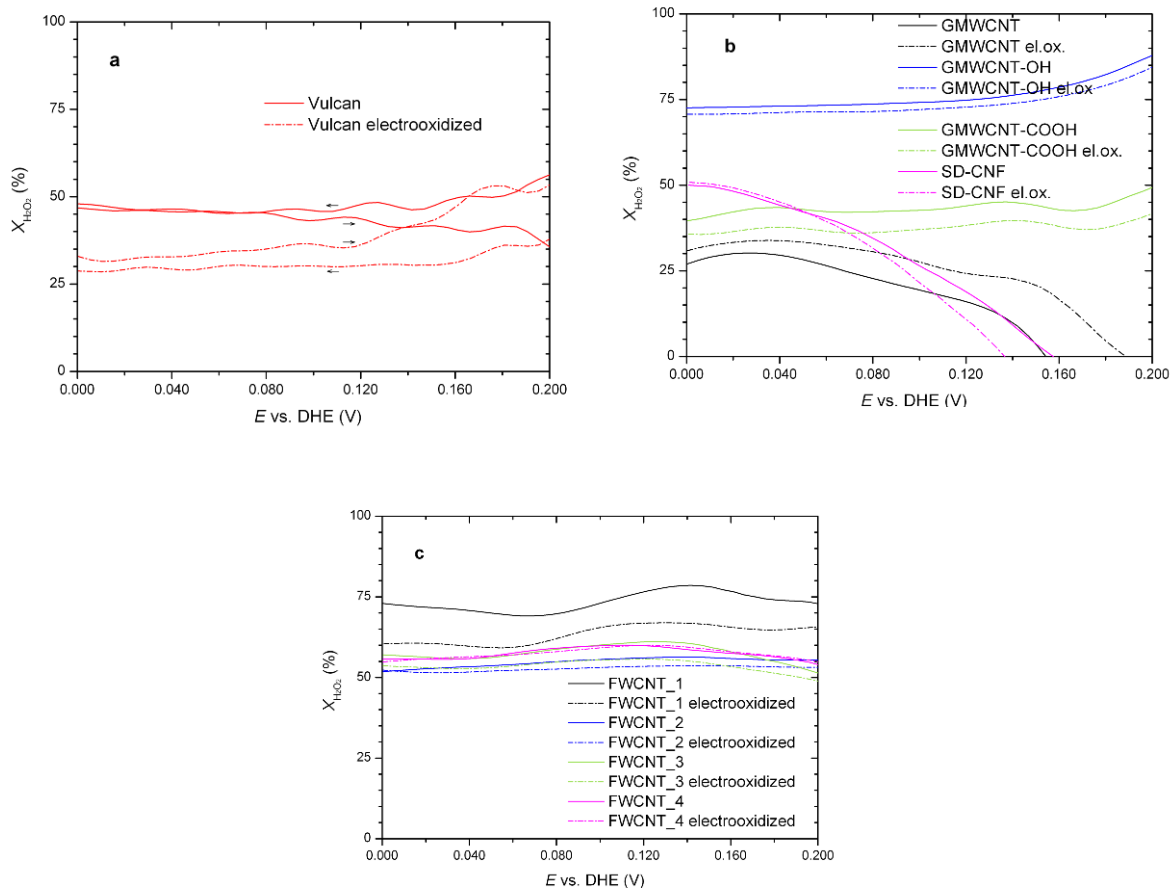

Figure 3.6. Percentages of peroxide formed in the range of 0-200 mV vs. DHE on thin-film electrodes of (a) Vulcan, (b) GMWCNTs and GNFs (SD-CNF), and (c) FWCNTs before (solid lines) and after (dash-dotted lines) five cycles between 0 and 1700 mV. 0.50 M $HClO_4$ electrolyte, 20 mV s^{-1} scan, 1500 rpm rotation. Positive-going sweeps for all samples; negative-going sweep included for Vulcan (sweep direction indicated by arrows).

It can be seen from Figure 3.6 (a) that X_{H202} for the Vulcan and electro-oxidized Vulcan is fairly constant within the depicted potential range. Also, in the lower end of the range there was not much difference between X_{H202} for the two sweep directions. On the non-oxidized Vulcan electrode approximately 45 mol% of the reduction products was peroxide, whereas after electro-oxidation this percentage was rather 30-35 mol%.

In Figure 3.6 (b), significantly more peroxide was generated on GMWCNT-OH than on GMWCNT, GMWCNT-COOH, and GNF. The ORR was found to be rather significant on this sample, so it seemed that the hydroxyl groups promoted the ORR, but mainly with peroxide as the product. For the unoxidized, graphitized GMWCNT and GNF, on the contrary, X_{H202} was seen to rapidly decrease as the potential was raised, which indicated that graphitization lowers the peroxide generation. Defects and hydroxyl groups, on the other hand, may promote peroxide generation.

For the FWCNT samples, Figure 3.6 (c), X_{H202} is nearly constant with potential, and also between the samples; only FWCNT_1 showed a somewhat higher X_{H202} than the others.

4 Catalyst synthesis

4.1 Pt deposition performed at VTT

4.1.1 Impregnation method

The catalyst nanoparticle synthesis was carried out by following a reproduced version of a method described by Bönnemann et al. (1994)[5]. This method is based on chemical reduction of metal salts with hydrotriorganoborates. In the platinum synthesis employed, $PtCl_2$ was used as the metal salt, and $Li[BEt_3H]$ as the reducing agent. Some alloy catalysts were synthesized as well, by combining Pt with base metals Co and Cr. The nanoparticle synthesis was combined with the catalyst synthesis by impregnating the support material with metal precursors in the solvent.

The Pt deposition by impregnation was performed on different types of GNFs and GMWCNTs. GNFs were divided in three groups: untreated fibers, acid treated fibers, and PANI treated fibers. Table 4.1 summarizes the samples synthesized by the impregnation method giving their sample codes, used support material, and the target amount of metal loading.

Table 4.1. Pt and Pt alloy catalyst samples synthesized by the impregnation method at VTT.

Sample code	Support	Target loading (wt%) (Pt unless mentioned otherwise)
MP023	untreated GNF	20
MP024	GMWCNT	20
MP028	untreated GNF	20 (Pt-Co 1:1)
MP029	untreated GNF	20 (Pt-Co-Cr 1:1:1)
MP030	untreated GNF	20 (Pt-Co 3:1)
MP031	untreated GNF	20 (Pt-Co-Cr 2:1:1)
MP032	untreated GNF	30
MP033	untreated GNF	40
MP034	GNF-005 (H_2SO_4 treated (8 h, 120 °C) GNF)	30
MP035	GNF-006 (HNO_3 treated (8 h, 120 °C)GNF)	30
MP036	GNF-007 (H_2SO_4/HNO_3 treated (8 h, 120 °C) GNF)	30
MP037	SD+10xPANI_600°C	20
MP038	SD+10xPANI_800°C	20
MP042	SD+3xPANI_800°C	20
MP043	SD+3xPANI_900°C	20
MP045	GMWCNT	20
MP046	GMWCNT-OH	20
MP047	GMWCNT-COOH	20

Impregnation method proved to be a very fast and convenient technique for depositing desired amounts of Pt on various supports, but the particle size was not fully controllable.

4.1.2 Organometallic synthesis

Another, completely different approach to Pt deposition was an organometallic synthesis of Pt phthalocyanines (PtPc) onto GNFs. The aim was to prepare platinum phthalocyanine (see Figure 4.1), attach it to a carbon support and subject the PtPc-carbon complex to pyrolysis in the same manner as was done in the PANI treatment. It was conceived that the phthalocyanine macrocycles could keep the platinum nuclei apart sterically

[5] Bönnemann, H., Brijoux, W., Brinkmann, R., Fretzen, R., et al. 1994. Journal of Molecular Catalysis 86, 1-3, pp. 129-177.

on the surface of the carbon support. PtPc had already been coated on carbon supports[6], but the final step of pyrolysis of the carbon supported PtPc catalyst was a new concept. However, a corresponding procedure was already known for e.g. cobalt phthalocyanine (CoPc)[7]. PtPc had been noted to catalyze the reduction of molecular oxygen to water directly without significant formation of hydrogen peroxide[8]. The synthesis of PtPc and PtPc/GNF materials were conducted by Ronnie Wahlström at VTT in Espoo, Finland.

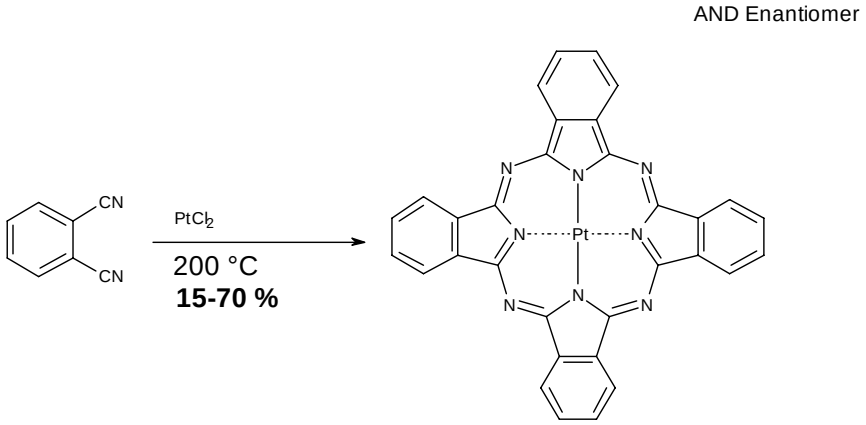

Figure 4.1. Synthesis of platinum phtalocyanine.

Two samples were prepared for further characterization: one directly synthesized PtPc/GNF sample and one PtCoPc/GNF sample, as presented in Table 4.2. The latter was synthesized by depositing platinum on a CoPc/GNF sample by the impregnation method.

Table 4.2. Phtalocyanine samples.

Sample code	Support	Target metal loading (wt%)
MP048	GNF	20 (Pt)
MP054	CoPc/GNF	15.5 (Pt-Co 1:3)

4.2 Pt deposition performed at Aalto University

Different methods were studied in order to deposit Pt particles on the carbon supports. Electrochemical deposition of Pt on SWCNT films was carried out by electrochemically reduction of H_2PtCl_6 precursor at -0.3 V vs. Ag/AgCl reference electrode. Even though the method proved to be fast and convenient, the particle size was observed to be very large (around 100 nm) and the particle size distribution was not controllable.

Impregnation method was also employed in order to deposit 20 wt% Pt on FWCNTs and GNFs. This was executed by the impregnation of H_2PtCl_6 on the support and subsequent reduction to metallic Pt by hydrogen flow at high temperatures. This method led to much larger Pt particle size and needless internal decoration of the tubes and fibers, as these catalyst particles would not be accessible for the ORR reaction.

Also colloidal polyol method was used to deposit 20 wt% Pt on FWCNTs and GNFs, including GNFs acid treated at VTT. The method consisted of the reduction of H_2PtCl_6 precursor to metallic Pt by ethyleneglycol in presence of the carbon support in alkaline media. By polyol method a high dispersion of particles and around 2-3 nm particle size were achieved. The stability of Pt/FWCNT and Pt/GNF during ultrasonic treatment was tested, showing that GNFs were more stable than FWCNTs.

[6] Brown, R. J. C., Kucernak, A. R., Long, N. J., Mongay-Batalla, C. New J. Chem. 2004, 28, 676-680.
[7] Lalande, G., Tamizhmani, G., Cote, R., Dignard-Bailey, L., Trudeau, M. L., Schulz, R., Guay, D., Dodelet, J. P. J. Electrochem. Soc. 1995, 142, 1162-1168.
[8] Shukla, A. K., Paliteiro, C., Manoharan, R., Hamnett, A., Goodenough, J. B. J. Appl. Electrochem. 1989, 19, 105-107.

4.3 Pt deposition performed at NTNU/SINTEF

4.3.1 Incipient wetness impregnation

In this technique the support material was dispersed in a mixture of isopropanol and water and was heated at 80 °C while refluxing. The solution was stirred and platonic acid was added dropwise to prevent the aggregate formation. Dissolved sodium borohydride in isopropanol was added at this stage. The final pH was set to be around 4 and the catalyst was collected using a filtration paper and washed several times to reach the neutral pH before drying at 90°C for 8 hours. The results showed that this method would not offer a proper control over the particle size and aggregate formation so it was decided to change the synthesis technique.

4.3.2 Polyol method

In this technique support materials and reducing agent were dispersed in ethylene glycol and were kept at 50 °C for ½ hour. While nitrogen was flowing in the reactor, platonic acid dissolved in ethylene glycol was added to the mixture whilst the temperature was increased to 110 °C. The mixture was kept at elevated temperature for 1.5 hours followed by cooling step in air and centrifuging the catalyst, ultrasonic homogenization and washing with hot water and acetone. The sample was dried at 80 °C for 8 hours to shape the final catalyst. The results were more promising than materials produced by the impregnation method but still far away from perfect, especially in terms of platinum particle size distribution.

4.3.3 Modified polyol method

To achieve the best results and establish the desired synthesis technique the polyol technique was modified both in the sequence of steps and process conditions. The processing temperature was increased up to 150°C. To improve the synthesis method it was found that doubling the amount of reducing agent, changing the sequence of mixing i.e. adding support material separately after platonic acid and increasing the duration of heating to 3 hours were notably effective. Washing with hot water was neglected as well. In this method platinum nanoparticles were prepared without using capping agents. 1.0 g of H_2Ptcl_6 was dissolved in 250 ml of ethylene glycol followed by addition of 100 ml of 0.5 M NaOH in ethylene glycol to maintain the pH slightly basic. Later, the prepared mixture was heated at 145 °C for 4 hours. Nitrogen was kept flowing on the solution in the course of reaction.

After this step, for the deposition of Pt nanoparticles on carbon material, the support was suspended in ethanol by ultrasonication of 15 min. Later the known volume of metal colloidal solution was added to the above suspension and pH of the mixture was adjusted to be approximately 2 by adding 1 M HCl, and sonicated for another 10 min. The above mixture was being stirred at 55 °C for 18 hours by bubbling N_2 in to the suspension. The solution was cooled down and centrifuged. The catalyst was washed repeatedly with acetone and finally with water and dried at 70°C for 8 hours. The same batch of Pt colloidal solution was used to deposit on different carbon materials.

The modified polyol method proved to be ideal to produce carbon supported platinum nanoparticles with varying metal loadings on various types of support. Moreover, it enabled an appropriate control over the particle size while it gave an option to synthesize completely aggregates-free samples, which was not possible by other techniques.

As a conclusion of the catalyst synthesis, different synthesis techniques were trialed to find the most promising method to synthesize carbon supported platinum catalysts. In this matter a vast variety of samples from 10 wt% to 40 wt% platinum loading on different carbon supports was synthesized. (Modified) polyol method proved to be the most capable synthesis technique among others applied. Conventional and modified polyol methods and impregnation were used to synthesize Pt/C samples with carbon black, carbon nanofibers and few-walled carbon nanotubes as supports.

5 Catalyst characterization

5.1 Physical methods

A complete package of physicochemical analysis as well as electron microscopy was performed to make sure that the samples were as desired in terms of the metal loading as well as structural homogeneity.

5.1.1 XRD and TGA

X-ray diffraction (XRD) was mainly used for determining the platinum particle size, but also for identifying the composition of the sample after the platinum deposition; in other words verifying the absence of undesired metal residuals. Thermogravimetric analysis (TGA) was used to examine the actual metal content of the samples. Table 5.1 summarizes the results of XRD and TGA analyses performed at VTT.

Table 5.1. Results of the XRD (average metal particle size) and TGA (metal content) analyses conducted at VTT.

Sample code	Sample description with target metal loading	Av. particle size (nm)	Metal content (wt%)
MP006	20 wt% Pt on GNF	2.6	13.4
MP008	20 wt% Pt on GNF	3.2	20.4
MP023	20 wt% Pt on GNF	3.8	20.2
MP024	20 wt% Pt on MWGNT	3.1	19.8
MP028	20 wt% Pt-Co (1:1) on GNF	4.9	12.0
MP029	20 wt% Pt-Co-Cr (1:1:1) on GNF	3.9	16.1
MP030	20 wt% Pt-Co (3:1) on GNF	4.4	15.6
MP031	20 wt% Pt-Co-Cr (2:1:1) on GNF	3.1	14.6
MP032	30 wt% Pt on GNF	6.8	26.6
MP033	40 wt% Pt on GNF	5.6	33.5
MP034	30 wt% Pt on GNF-005	4.6	25.3
MP035	30 wt% Pt on GNF-006	5.7	27.0
MP036	30 wt% Pt on GNF-007	4.1	25.4
MP037	20 wt% Pt on SD+10xPANI_600°C	4.6	16.5
MP038	20 wt% Pt on SD+10xPANI_800°C	4.5	16.2
MP042	20 wt% Pt on SD+3xPANI_800°C	3.9	15.6
MP043	20 wt% Pt on SD+3xPANI_900°C	5.3	16.4
MP045	20 wt% Pt on GMWCNT	4.3	17.8
MP046	20 wt% Pt on GMWCNT-OH	5.8	22.2
MP047	20 wt% Pt on GMWCNT-COOH	5.9	21.0
MP048	20 wt% Pt in PtPc/GNF	-	21.9
MP054	15.5 wt% Pt-Co in Pt/CoPc/GNF	-	7.2

It can be observed that the target metal loading was realized rather well in samples of 20 wt% loading target. In the first samples the process was not fully optimized, and the metal content remained low in some cases, e.g. in sample MP006. Only metal alloy samples, MP028-031, presented values that were clearly lower than the target, implying that the synthesis of multi-metal samples was not as controlled as the plain platinum synthesis. Also targets higher than 20 wt% were not completely realized as can be seen in samples MP032 and MP033. Acid treatment (samples MP034-036) did not seem to cause a significant change in realized metal content compared to untreated sample with similar metal target loading (MP032). On the contrary, acid treatment seemed to slightly decrease the platinum particle size. Metal loading remained lower than target in all PANI treated samples, MP037-038, MP042-043. Oxygen functionalities seemed to increase the platinum

particle size in GMWCNT samples, MP045-047. The depositing of Pt on CoPc/GNF did not succeed and the achieved metal loading remained in half of the targeted.

Similarly, the samples synthesized and characterized for Pt particle size and loading at Aalto University are presented in Table 5.2.

Table 5.2. Results of the XRD (average metal particle size) and TGA (metal content) analyses conducted at Aalto University.

Sample notation	Av. Pt particle size (nm)	Pt loading (wt%)
TKK-Pt/GNF	3.0	15
TKK-Pt/Ox-GNF	3.5	18
TKK-Pt/VGF	2.8	20
TKK-Pt/Ox-VGF	1.8	11
Pt/FWCNT_1	2-4	15
Pt/FWCNT_2	2-4	19
Pt/FWCNT_3	2-4	18

A reference catalyst by BASF Fuel Cell inc. was characterized as well. The sample consisted of nominally 20 wt% Pt on Vulcan XC-72 carbon black. The actual Pt loading was observed to be approximately 19.8 wt% and average Pt particle size 2.5 nm. This sample will be in future referred to as "BASF" according to the manufacturer.

5.1.2 SEM and TEM imaging

Aalto carried out structural and morphological characterization of Pt/FWCNTs, Pt/SWCNTs and Pt/GNFs prepared by various methods both by Aalto and other partner institutes, by transmission electron microscopy (TEM) and scanning electron microscopy (SEM) to determine the Pt size and distribution on the carbon supports. Some representative TEM and SEM images of the materials prepared by different methods on different carbon supports are shown in Figure 5.1.

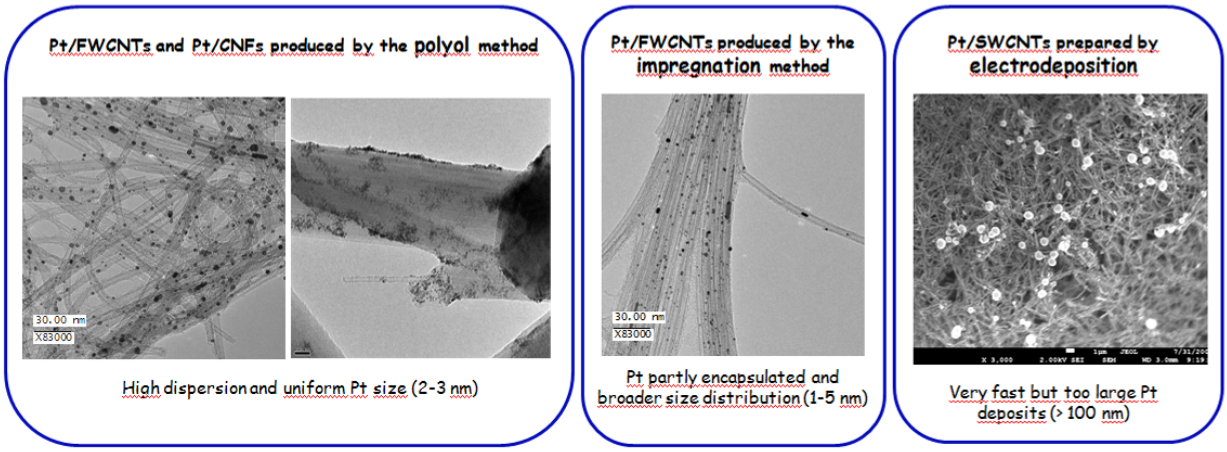

Figure 5.1. TEM and SEM images of Pt/FWCNT and Pt/GNF prepared by the polyol (left), impregnation (centre) and electrochemical (right) methods.

A batch of four catalyst materials including samples with theoretical loading of 20 wt% of Pt on both functionalized and unfunctionalized carbon nanofibers was prepared. The actual loadings were determined by energy dispersive spectroscopy (EDS). Figure 5.2 shows TEM images of the four samples.

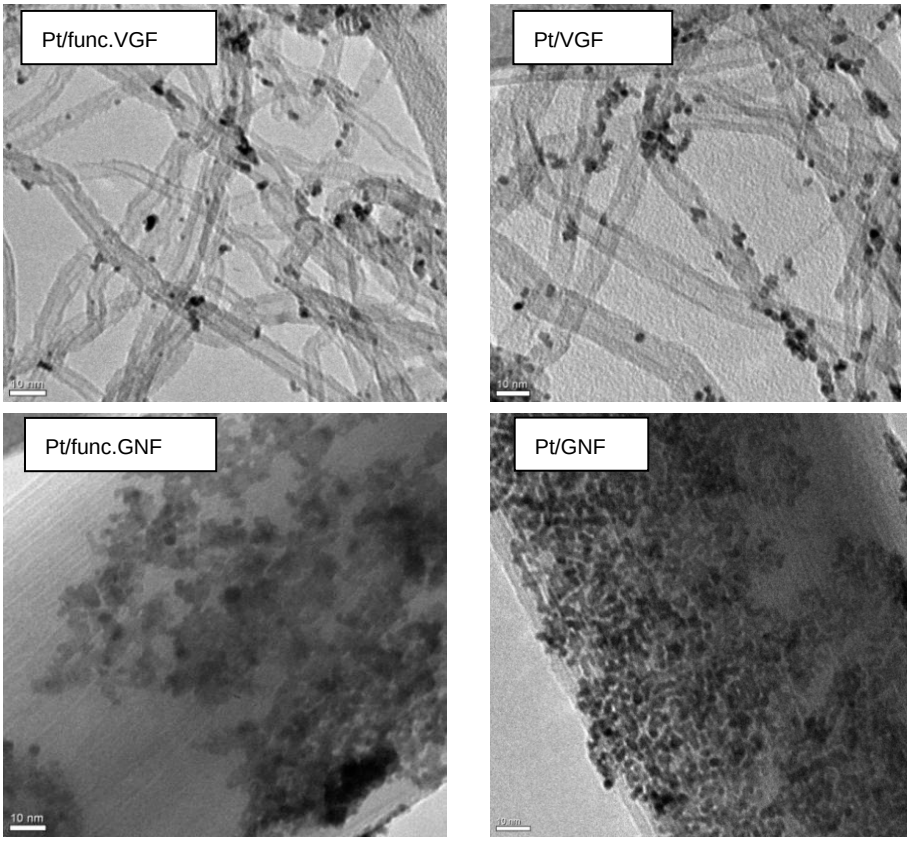

Figure 5.2. TEM images of Pt/VGFs and Pt/GNFs synthesized at Aalto University for degradation studies.

Samples synthesized by the modified polyol method at NTNU appeared to contain only individual particles and had a high homogeneity and uniform dispersion in the support matrix, see Figure 5.3. Pt particle size was estimated to be less than 2 nm in these samples.

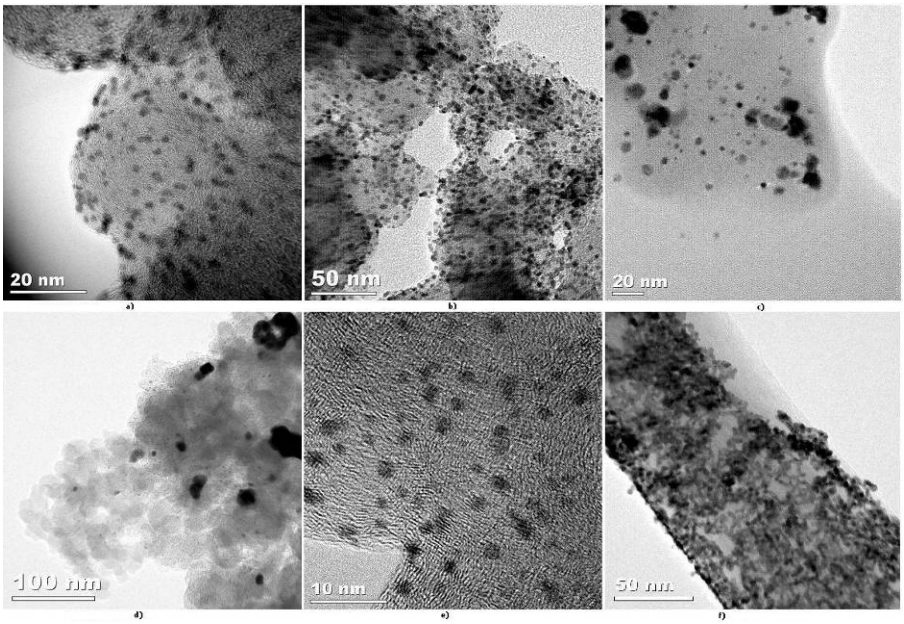

Figure 5.3. TEM images of the samples a) 20 wt% Pt/Vulcan by adsorption polyol b) 30 wt% Pt/Vulcan by adsorption polyol c) 10 wt% Pt/Vulcan by polyol d) 15 wt% Pt/Vulcan by polyol e) 10 wt% Pt/Vulcan by adsorption polyol f) 23 wt% Pt/GNF by polyol.

5.2 Electrochemical methods

As soon as the synthesis method was established and the desired outcome of the synthesis was preliminary confirmed by physical methods, the catalysts were characterized electrochemically. To do this, regular CV and CO stripping voltammetry among other methods were employed to understand and determine the electrochemical performance of the electrocatalysts and to acquire valuable information e.g. of the presence of aggregates or individual particles.

5.2.1 *In situ* active area determination at KTH

In the evaluation of catalyst materials for PEMFC it is valuable to be able to determine the catalyst active area *in situ*. With the increased focus on degradation, it is even more important to make an accurate determination of the changes in active area before and after degradation tests. It is generally considered that a good estimation of the platinum active area can be made from the hydrogen underpotential deposition (H_{upd}) charge. Another common method for the determination of the active area is to use stripping of an adsorbed CO monolayer. The charge of the oxidation peak is generally taken to be equivalent to two electrons per CO molecule, which results in a charge about twice that of the H_{upd} peak. Because these methods were originally defined in an acidic solution, the effect of *in situ* environment, such as temperature and humidity, was investigated[9]. Some results are presented in Figure 5.4 and Figure 5.5.

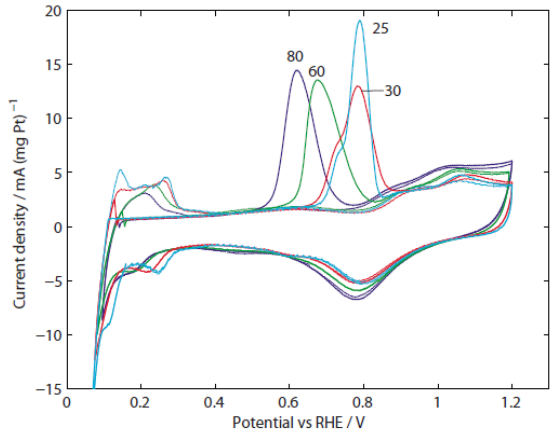

Figure 5.4. CV and CO stripping for 20 wt% Pt/Vulcan recorded at a sweep rate of 10 mV/s. Gases at 90% RH. The cell temperatures in °C are indicated in the figure.

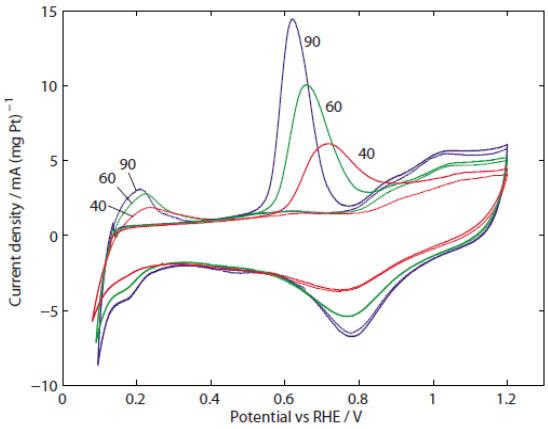

Figure 5.5. CV and CO stripping for 20 wt% Pt/Vulcan recorded at a sweep rate of 10 mV/s. Cell temperature at 80 °C. The different relative humidities are indicated in the figure.

The charges of the hydrogen underpotential deposition (H_{upd}) and CO stipping peaks obtained *in situ* were compared, and the influence of operation temperature (25–80 °C) and relative humidity (40–90 %) was discussed. The results showed that the charges of the H_{upd} decreased with rising temperature, while the corresponding charges of the CO stripping peak were essentially independent of temperature, at least at high relative humidity. The unexpectedly small H_{upd} charges were explained by the significant overlap with the hydrogen evolution reaction in a fuel cell at elevated temperatures. However, with decreasing humidity the charges of both H_{upd} and CO stipping peaks decreased, which was probably an effect due to increasing blockage of Pt active sites by hydrophobic domains in the electrode ionomer.

The varying cell conditions on the estimated Pt active area and its correlation with fuel cell activity may also have important implications when performing accelerated degradation tests (ADT). During the evaluation of alternative carbon materials as support for the Pt catalyst in PEMFC, very high electrode potentials may be applied to the electrodes as a part of the ADT to evaluate the material stability. Repeatedly high potential excursions may temporarily dry out the electrode due to the ongoing water oxidation. Figure 5.6 shows that a reversible degradation may be accounted for, when determining the active surface area of the catalyst from H_{upd}, if not sufficient recovery time is considered after the ADT. It was concluded that both the parameter study

[9] Rakel Wreland Lindström, *Journal of The Electrochemical Society*, 157(12) (2010) B1795-B1801

and the accelerated degradation test showed that CO stripping is less affected by, and better defined at, various fuel cell conditions than the H_{upd}. As the H_{upd} is close to the potential for the on-set of hydrogen evolution, an overlap between these reactions cannot be avoided. It was therefore proposed that CO stripping is a more accurate measure of the active area in a fuel cell. If the H_{upd} area will be used, a relatively good estimation is achieved when the temperature is decreased to room temperature and water saturated gases at a very low or, preferably, zero flow rates are used.

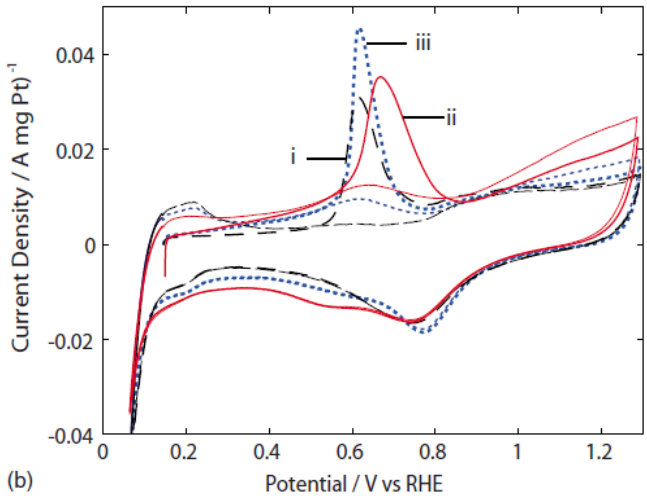

Figure 5.6. CO stripping curves at a sweep rate of 10 mV/s, (i) before, (ii) after 3 h at 1.4 V, and (iii) after 12 h at rest at room temperature.

5.2.2 Experimental work at SDU

5.2.2.1 Hydrogen adsorption/desorption coulometry

The determination of the electrochemical surface area was made by determining the hydrogen sorption of four different catalyst loadings of the RDE (7-30 µg/cm^2). From this the roughness factors could be determined. By plotting the roughness factors, r_f, vs. catalyst loading a linear relationship emerged, see Figure 5.7, from which the slope was the ECSA per weight of platinum.

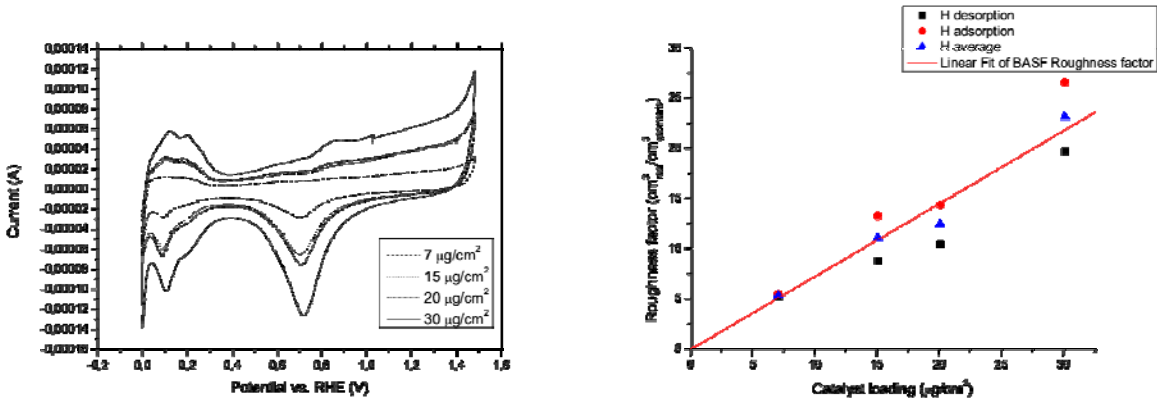

Figure 5.7. CVs of RDE containing BASF Pt on Vulcan with different loadings (7-30 µg/cm^2) (a) and the roughness vs. loading plot used for determining the ECSA slope (b).

The electrochemical CV experiments were made using a Zahner IM6eX electrochemical workstation (Zahner-Electric GmBH & Co.KG, De) controlled by Thales 1.48 program, or an IviumStat electrochemical interface (Ivium Technologies B.V., Nl) controlled by a computer using IviumSoft 1.420.

The dual electrode cyclic voltammetry (DECV) experiments were made on a Pine AFCBP1 bipotentiostat (Pine Research Instruments, NC USA) controlled by using Aftermath 1.2.4361.

The rotating disc electrode setup consisted of an AFMSRXE modulated speed rotator from Pine Research Instruments with an E5 interchangeable RDE tip with a 5.0 mm diameter mirror polished glassy carbon (GC) electrode surface.

The ECSA for the provided catalysts were determined by the four electrode loadings described. The ECSA per weight of platinum are summarized in Table 5.3. The determination of the ECSA for the polyaniline treated samples MP042-043 was done from only the two highest loaded catalyst electrodes, as the platinum signals were impossible to distinguish from the pseudo capacitance of the support at loading <20 μg/cm^2.

Table 5.3. Electrochemical surface areas of catalyst samples determined by thin film RDE method.

Sample code / notation	Sample description	Calculated area (m^2/g_{Pt})	Determined ECSA (m^2/g_{Pt})
BASF	20 wt% Pt on Vulcan	112.1	72.7
MP006	20 wt% Pt on GNF	107.8, 133.5	27.39
MP008	20 wt% Pt on GNF	87.6, 133.5	17.46
MP032	30 wt% Pt on GNF	41.23	18.56
MP033	40 wt% Pt on GNF	50.06	16.88
MP034	30 wt% Pt on GNF-005	60.95	24.69
MP035	30 wt% Pt on GNF-006	49.18	17.57
MP036	30 wt% Pt on GNF-007	68.38	28.38
MP042	20 wt% Pt on SD+3xPANI_800°C	71.89	11.95
MP043	20 wt% Pt on SD+3xPANI_900°C	52.90	27.93
MP045	20 wt% Pt on GMWCNT	65.20	6.7[10]
MP046	20 wt% Pt on GMWCNT-OH	48.34	2.6[10]
MP047	20 wt% Pt on GMWCNT-COOH	47.52	1.2[10]
MP048	20 wt% Pt in PtPc/GNF	-	35.2
MP054	15.5 wt% Pt-Co in Pt/CoPc/GNF	-	-
TKK-Pt/GNF	-	93.46	41.78
TKK-Pt/Ox-GNF	-	80.11	39.22
TKK-Pt/VGF	-	100.1	74.68
TKK-Pt/Ox-VGF	-	155.8	19.56
Pt/FWCNT_1	-	140-70	34[10]
Pt/FWCNT_2	-	140-70	13[10]
Pt/FWCNT_3	-	140-70	21[10]

By the table above it can be seen that the ECSA of the BASF sample was among the highest. The highest ECSA was achieved by the polyol platinized carbon fibers TKK-Pt/VGF, which however were found to be less stable to corrosion than the standard BASF catalyst. MP043 catalyst seemed to have a high ECSA. However, as the determination of the ECSA was made from only two of the catalyst loaded electrodes with some extent of uncertainty, as the platinum features were nearly indistinguishable from the capacitance layer. The ECSA of these samples are highly questionable.

The samples MP034 and MP036 appeared to be good candidates for further testing under working fuel cell conditions. However, when comparing the physical determinable areas, these samples exhibited half of the potentially possible electrochemical surface area. These samples could be modified for better fuel cell ECSA by tweaking the platinization parameters.

The samples determined by M. J. Larsen during his PhD all have lower ECSA. It should be noted that the electrochemical cleaning process employed, sweeping from 0 to 1.3 V, is more delicate than electrochemically sweeping to 1.48V. Therefore the measured ECSA is after the former cleaning process about half compared to

[10] Determined by Mikkel J. Larsen during his PhD work.

the latter method. The ECSA determined from the Pt/FWCNT_1 is therefore comparable to the platinum catalyst reference BASF. The remaining two Pt/FWCNT catalysts both have decent ECSAs when normalized, whereas the GMWCNT samples MP045-047 exhibit exceptionally low determinable ECSAs.

As a conclusion, the catalysts platinized by the impregnation method exhibited low to medium ECSAs. The catalysts with GMWCNT and functionalized GMWCNT exhibited the extreme lowest ECSA. The platinum phtalocyanine platinized catalysts exhibited highly questionable ECSA of up to 35 m^2/g_{Pt}. The highest determinable ECSAs were those of polyol platinized catalysts.

5.2.2.2 Nafion ionomer and carbon/carbon based catalyst interaction

Partial experiment regarding Nafion ionomer and carbon, or Nafion and carbon based catalyst interaction was conducted.

The procedures were based on earlier work[11]. The basic idea of the work was mixing the ionomer and carbon or catalyst in aqueous solution. Based on concentration change of the ionomer (detected by ^{19}F nuclear magnetic resonance spectroscopy (NMR)), the degree of the affinity between the ionomer and particles were interpreted. An example of Nafion ionomer ^{19}F-NMR spectrum is shown in Figure 5.8.

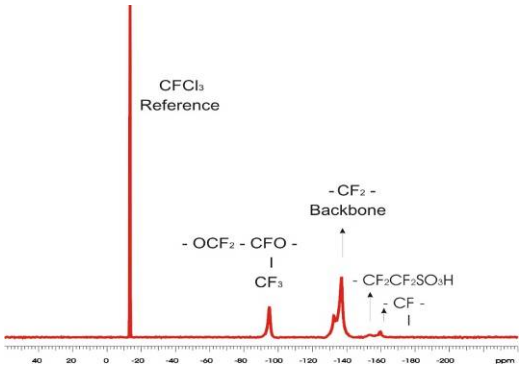

Figure 5.8. ^{19}F-NMR of Nafion ionomer.

Based on the preliminary results, an indication that carbon nanofiber based catalyst has stronger interaction with Nafion ionomer comparing to CNT and Vulcan based catalyst, was observed.

5.2.3 Experimental work at NTNU/SINTEF

5.2.3.1 CO stripping

CO stripping voltammetry was performed at different sweep rates to examine the electrochemical performance of the catalysts and the possible presence of aggregates. In this experiment CO adsorption was carried out from the CO saturated 0.5 M $HClO_4$ solution at an adsorption potential of 50 mV for 120 seconds and the excess of CO dissolved in the solution was removed by purging Ar for 30 min while the electrode was fixed at the adsorption potential. Figure 5.9 shows the CO stripping voltammograms for the samples of which TEM images have already been presented in Figure 5.3. It is well known that for the catalysts including only isolated particles there appears a single narrow CO oxidation peak while the appearance of two or more peaks at the CO oxidation region is a sign of agglomeration formation in the sample[12]. The CO stripping results were in a perfect agreement with the TEM images.

[11] Ma S. et al. Solid State Ionics, 178 1568-157, 2007.

[12] Maillard, F., Schreier, S., Hanzlik, M., Savinova, E. R., Weinkauf, S., & Stimming, U. (2005). Influence of particle agglomeration on the catalytic activity of carbon supported Pt nanoparticles in CO monolayer oxidation. *Physical Chemistry Chemical Physics*, *7*(2), 385. doi: 10.1039/b411377b

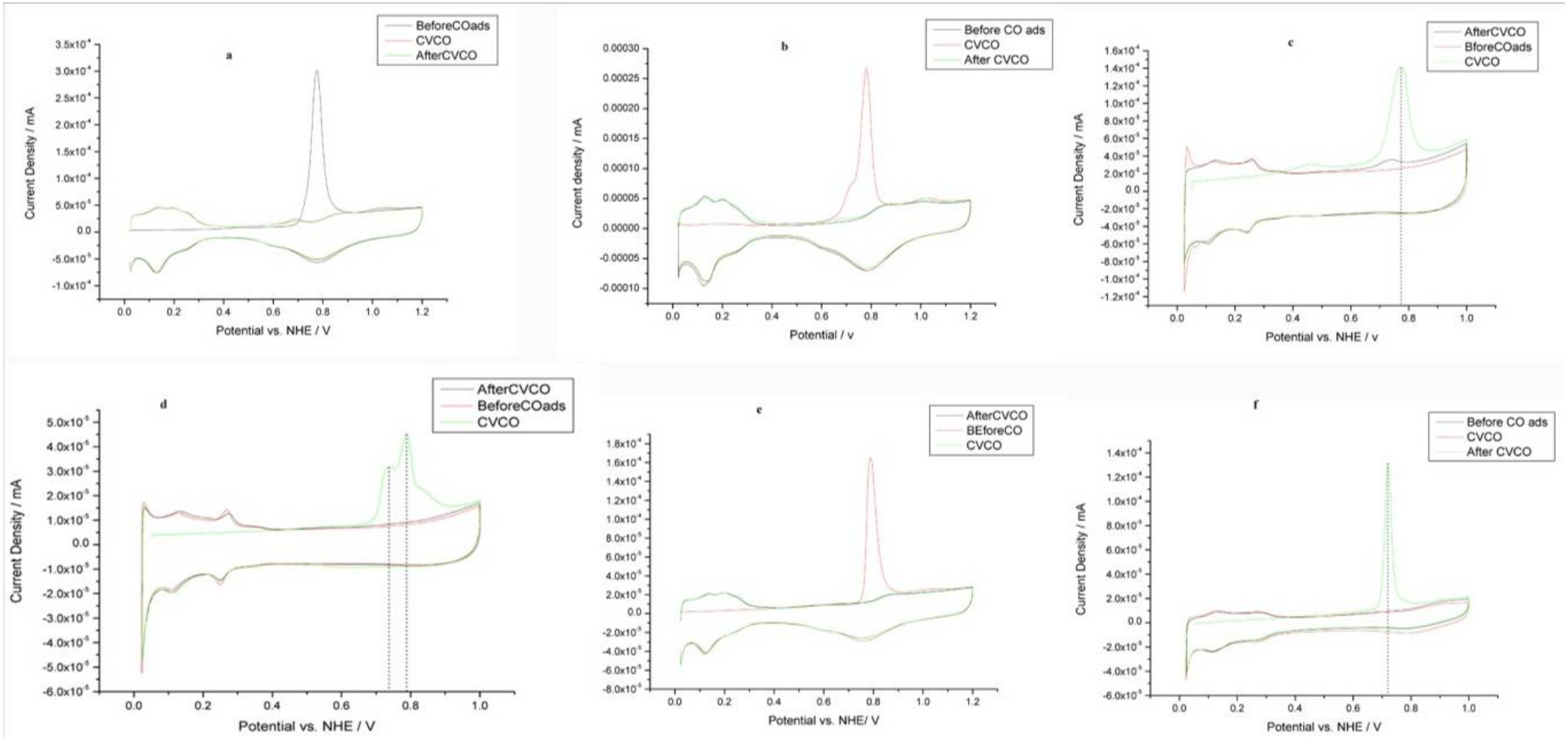

Figure 5.9. CO stripping voltammograms at a sweep rate of 10 mV s^{-1} for samples from a to f as mentioned in Figure 5.3. Ar was in working electrode compartment and 0.5 M $HClO_4$ in counter electrode compartment, the experiment carried out at room temperature.

5.2.3.2 Cyclic voltammetry of Pt

Noble metals such as Pt, Pd and Au have well defined hydrogen adsorption and desorption peaks seen upon cycling between suitable potential limits using the cyclic voltammetry technique. Due to these defined peaks several values can be determined for the Pt based catalysts. By analysis of the oxidation peaks a determination of the electrochemical surface area of catalyst can be determined.

The sample preparation for the cyclic voltammetry performed on RDE was conducted as follows. The catalyst layer was composed of a catalyst powder (e.g. 2.0 mg) dispersed in a solvent (e.g. 20 % isopropanol or ethanol in water). Consequently, 20 µl of the catalyst dispersion was taken with a pipette and put on a glassy carbon disk. After drying, a binder such as a dilute Nafion solution was added on the catalyst to avoid delamination of the catalyst layer during measurements.

Figure 5.10 and Figure 5.11 show an example of the cyclic voltammetry studies of Pt/C catalysts. In this case, the effect of electrolyte temperature on hydrogen adsorption peaks, and formation and reduction of Pt oxide was studied. It can be seen by the figures that the amount of adsorbed hydrogen decreases with increasing temperature, while the onset potential for oxide formation and reduction was shifted to higher potentials.

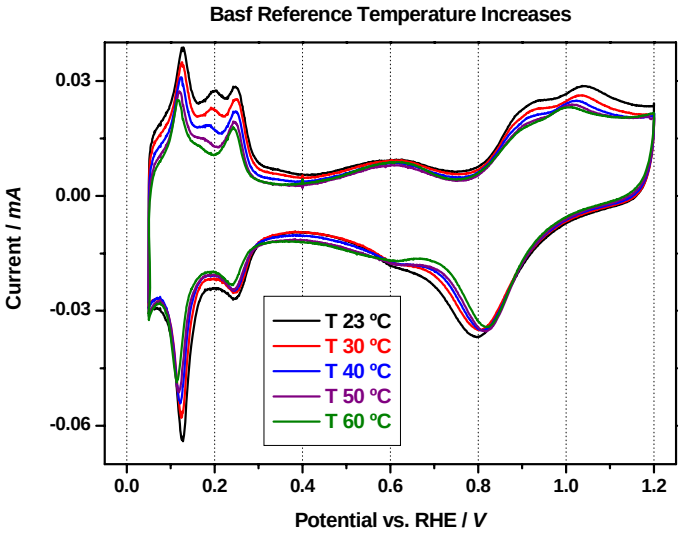

Figure 5.10. Cyclic voltammetry of Pt/C reference catalyst (BASF catalyst) in 0.5 M H_2SO_4 at different temperatures.

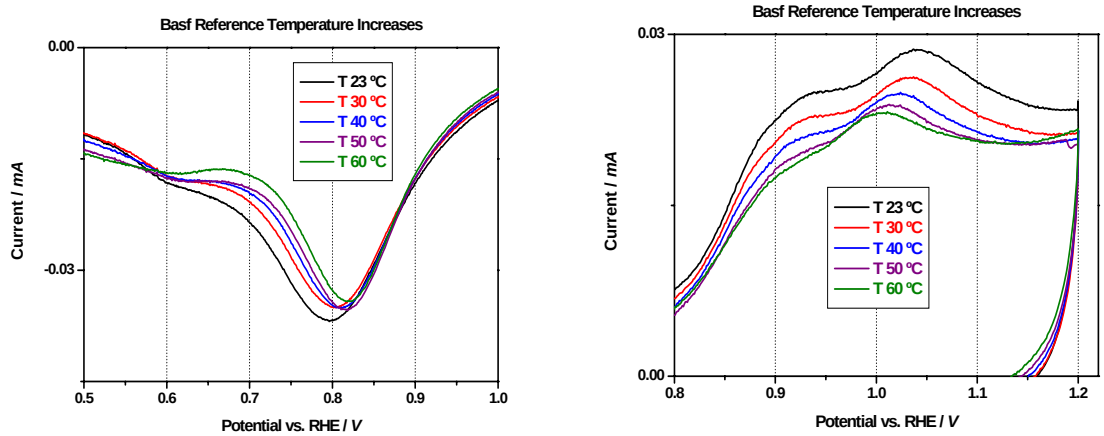

Figure 5.11. Pt oxide reduction peaks (left) and Pt oxide formation peaks (right) as a function of temperature for Pt/C reference catalyst in 0.5 M H_2SO_4.

Additionally, to know and quantify the electrochemical active area in catalytic systems based on Pt, CO is a useful probe in electrochemical platinum based catalysts characterization, blocking the Pt surface at low potentials (hydrogen region). The CO stripping procedure involves an electrochemical adsorption of carbon monoxide followed by electro-oxidation. The amount of CO adsorbed is estimated by stripping peak integration corrected for the charging of the double layer assuming that one CO monolayer its adsorbed linearly and the charge used for oxidizing is 420 μC cm^{-2} Pt. Additionally, the shape of the CO stripping voltammogram of a Pt catalyst is dependent on morphology, structure, size and chemical nature, and hence provides us with additional information about how the particles are dispersed on the support material, i.e. if they are aggregated or homogeneously dispersed.

Figure 5.12 shows an example of the CO stripping measurements. In this case, the effect of electrolyte temperature on the size and position of the CO stripping peaks were studied. It can be seen that at low temperature, the CO peak is divided into several sub-peaks indicating a small degree of Pt particle agglomeration in this catalyst. At higher temperatures however, the main CO peak shifts to more cathodic potentials, masking the smaller peaks. This indicates that *in situ* CO stripping measurements of catalysts in PEM fuel cells at elevated temperatures will not be able to detect Pt particle sintering.

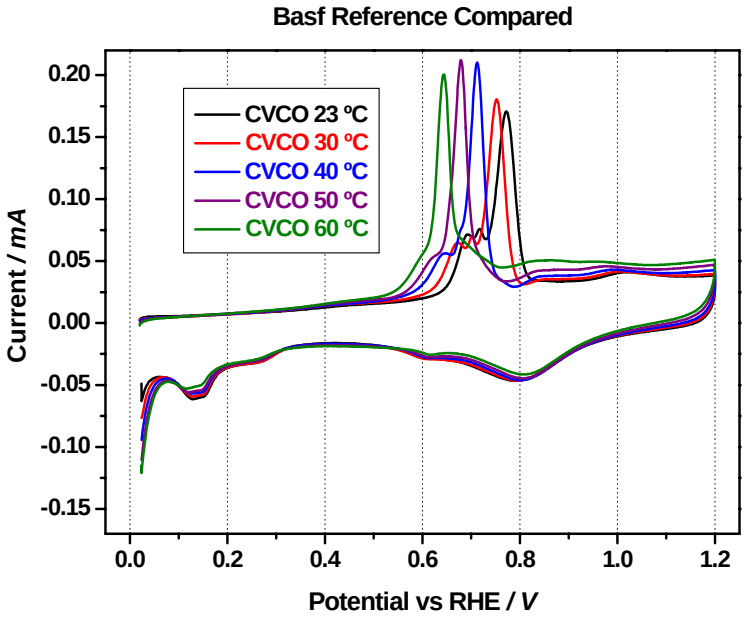

Figure 5.12. CO-stripping measurements of Pt/C reference catalyst at different electrolyte (0.5 M $HClO_4$) temperatures.

6 Catalyst durability studies

6.1 Experimental work at KTH

6.1.1 The electrochemical response of a carbon corroded cathode

Considerable attention has recently been paid to the issues concerning the corrosion of the catalyst support in PEMFC electrodes. Under normal fuel cell operation the catalyst support is believed to be stable and negligible fuel cell degradation due to carbon corrosion is assumed. However, under fuel starvation conditions it has been shown that the electrodes may reach high enough potentials to induce severe carbon corrosion. The carbon loss is reflected in the thinning of the electrode, loss of electrochemically active area due to Pt dissolution/isolation/agglomeration and severe degradation of the fuel cell performance, especially at high current densities. Furthermore, the degradation at high current densities is usually explained in the literature as mass transport losses in the catalyst layer due to i) flooding of the catalyst layer as the support becomes more hydrophilic upon its oxidation[13] and ii) decrease of the electrode porosity as the catalyst layer totally collapses[14,15].

Several electrochemical techniques such as cyclic voltammetry, CO stripping, electrochemical impedance spectroscopy and polarization experiments were implemented to investigate how the stability/instability of the carbon support affects the electrochemical response of the MEA under different RH of the gases and different partial pressures of oxygen. Additionally, SEM was implemented as a tool to correlate the changes in fuel cell performance with the changes in electrode morphology.

The Pt/Vulcan electrode showed in Figure 6.1 was submitted to an accelerated degradation test consisting of 300 cycles between 1.4 V and 0.6 V vs. RHE with a sweep rate of 40 mV/s. The cathode not only decreased in thickness, but as seen from the SEM images, it also underwent considerable changes in the electrode morphology. In some parts and especially at the gas diffusion layer/catalyst layer (GDL/CL) interface, the vital porous structure of the electrode completely collapsed.

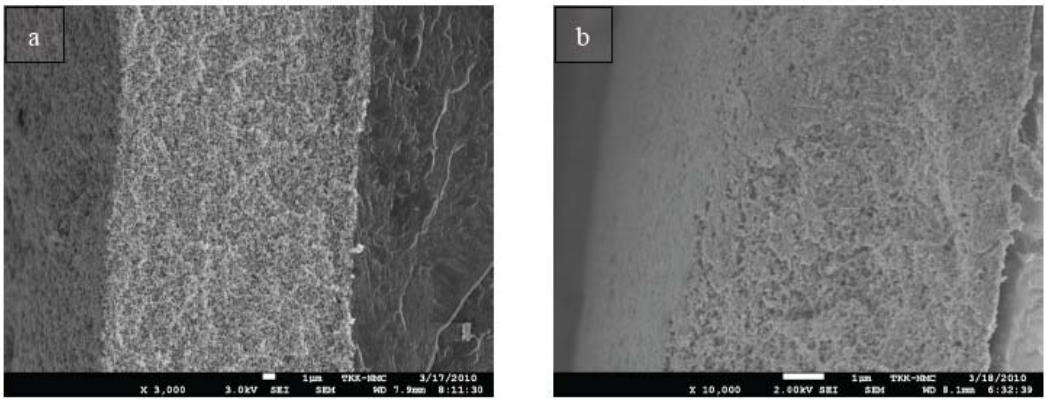

Figure 6.1. SEM-images of 20 wt% Pt/Vulcan before (a) and after degradation (b).

The electrodes for the experimental PEM fuel cell experiments were prepared by a drop electrode method[16]. The electrode ink was prepared by dispersing the sample powder in a solution consisting of 5 wt% Nafion solution, and equal volumetric amounts of deionized water and isopropanol. After sufficient stirring and ultrasonication, 20 µl of the electrode ink was pipetted on a purified Nafion 115 membrane and let dry at 90 °C. The MEA was finished by hot pressing a commercial gas diffusion electrode (ETEK, 30 wt% Pt on Vulcan XC-72) on the other

[13] R. Borup, Chemical Reviews, 107 (2007) 3904-3951
[14] P. T. Yu, ECS Transactions, 3 (1) (2006) 797-809
[15] Z. Y. Liu, Journal of The Electrochemical Society, 155 (10) (2008) B979-B984
[16] R. Wreland Lindstrom, K. Kortsdottir, M. Wesselmark, A. Oyarce, C. Lagergren, G. Lindbergh, *J.Electrochem.Soc.* **2010,** 157, B1795.

side of the membrane as the anode electrode. The prepared MEAs were tested in an experimental single cell controlled by Princeton Applied Research 263A potentiostat and Corrware software.

The electrochemical measurements of the degraded Pt/Vulcan electrode correlated very well with what was seen in the SEM images: i) decreased active surface area of Pt due to its agglomeration, ii) decreased catalyst layer resistance due to electrode thinning and increased volume fraction of ionomer and iii) increased mass transport resistance due to the decreased electrode porosity. The lack of porosity hindered the proper oxygen diffusion into and through the catalyst layer, especially under conditions where liquid water might be present in the electrode, e.g. at high RH and high current densities.

As it is showed in the polarization curves in Figure 6.2, at low RH and using pure oxygen, there was almost no degradation in fuel cell performance. At 0.5 A/cm^2 there was only a 1 % voltage decrease. Comparing instead the polarization curves at high RH, also using pure oxygen, the voltage decrease at 0.5 A/cm^2 was instead 15 % from the initial performance. Mass transport limitations in the cathode catalyst layer of a PEMFC are rarely observed using pure oxygen, therefore it was suggested that liquid water is probably blocking a large part of the few remaining pores at the GDL/CL interface. As the partial pressure of oxygen decreased, it was possible to observe the real extent of the degradation of the carbon support. When using air, there was indeed a significant degradation even at low RH. In this case the voltage was 13 % lower than its initial value at 0.5 A/cm^2; it was therefore suspected that the electrode itself was acting as a diffusion barrier. Finally, at high RH and using air, the performance degradation was certainly the worst: 34 % decrease in voltage at 0.5 A/cm^2.

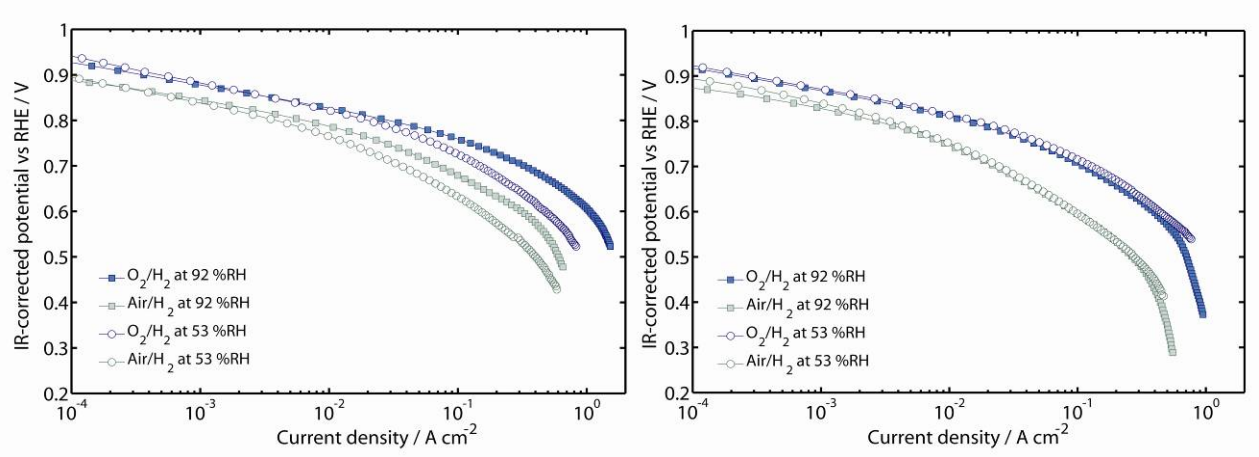

Figure 6.2. IR corrected polarization curves before (left) and after (right) the accelerated carbon corrosion test. Cell temperature: 80 °C and H_2 at the anode. The polarization curves were recorded using the same volumetric flow rate of both fuel and oxidant (60 ml/min) instead of equal stoichiometry to ensure the same water balance in the cell when comparing the performance of pure oxygen with air.

This study provided useful information enabling to identify performance degradation due to carbon corrosion. The study also gave an insight on the particular characteristics that alternative catalyst support should have. Vulcan XC-72 support has the tendency to agglomerate upon corrosion, decreasing the electrode porosity and increasing the mass transport limitations for all RHs. It was suggested that alternative catalyst supports should not only have a high corrosion resistance, but also have a low tendency to collapse upon repeatedly exposures to high potentials.

6.1.2 *In situ* durability studies of alternative carbon supports

Durability screening studies are usually carried out in simulated fuel cell environment (*ex situ*). In this study however, the durability of several intrinsically different carbon supported Pt electrodes were studied in real PEMFC environment (*in situ*) and compared to commercially available BASF catalyst.

To compare the materials in carbon stability in PEMFC, the electrodes were degraded under potential cycling (0.6-1.4 V vs. RHE) with a sweep rate of 40 mV/s in O_2 atmospheres at 80 °C and 90 % RH.

In this study, the cyclic voltammograms were viewed as fingerprint for the stability of each carbon material. No quantitative information was taken from the H_{upd} region due to reasons discussed earlier, however a qualitative analysis was able to provide important information about the stability of the materials.

As the carbon materials were oxidized due to the high potentials imparted by the degradation test, the double layer region (0.4-0.6 V vs. RHE) started to change. Reasons for an increased capacitance could be: i) oxygen functionalities on the surface of the carbon, ii) different types of defects and iii) a larger contact area between the electrolyte and carbon surface as the support became more hydrophilic. However, it was also showed that as the corrosion became significant and the carbon material was corroded to CO_2, the double layer capacitance started to decrease in magnitude again.

Figure 6.3. shows that all the materials tested showed an increase in double layer capacitance and that all the materials except the GNFs (c) and to some extent the GMWCNTs (e) showed a considerable increase in the double layer region, especially at around 0.6 V vs. RHE where the quinone/hydroquinone redox couple is active. Additionally, is it also possible to observe a large decrease in both the H_{upd} region at low potentials, as well as in the Pt oxidation and Pt reduction region at high potentials, indicating that there was considerably less Pt area available for the oxygen reduction reaction for all the catalysts, except for the GNFs (c), but especially for the FWCNTs (f).

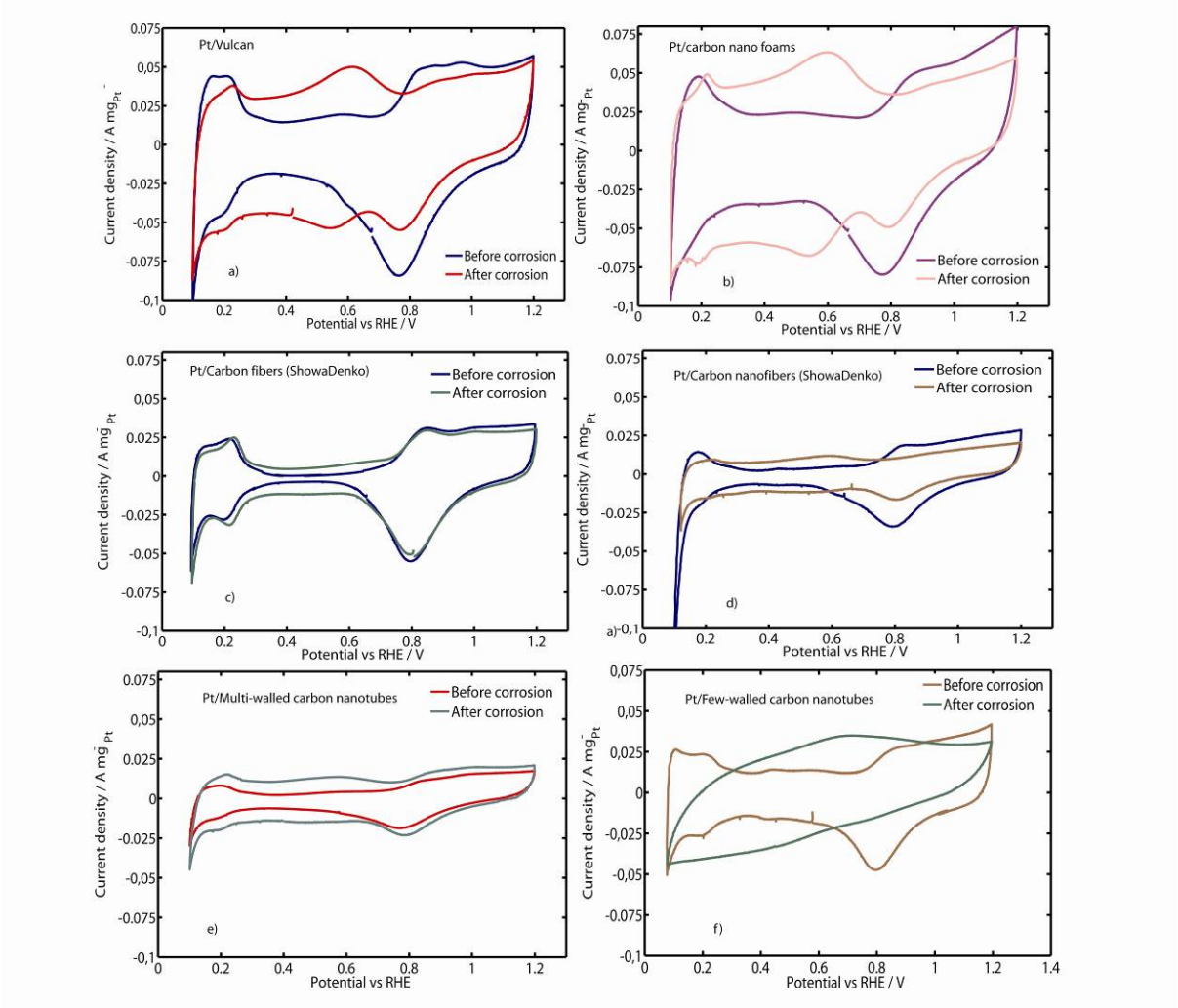

Figure 6.3. Cyclic voltammograms of cathodes before and after degradation test. The voltammograms are recorded at 80 °C, fully humidified N_2 at the cathode and fully humidified 5 % H_2 in Ar at the anode.

The polarization curves, see Figure 6.4, revealed that the alternative catalyst supports for PEMFC electrodes showed a wide range of different behavior. However, all of them showed little or no degradation at low current

densities. As discussed above, degradation due to carbon corrosion mainly affected high current densities, when the water production by the oxygen reduction reaction may block the diffusion path of oxygen, thus increasing mass transport resistances. The only catalyst that seemed to have lost all its activity was the FWCNT supported Pt. These carbon nanotubes are very fragile and susceptible for degradation. An effort was made to test different purification pretreatments without considerable success. The GMWCNT supported Pt electrodes on the other hand was the only material that showed a significant improvement over the entire polarization curve. It was suggested that this highly hydrophobic materials improved its contact with the Nafion ionomer as its surface was oxidized. However, the poor overall performance of this catalyst was not sufficient to make it a candidate for PEMFC electrodes. The Vulcan support (a) as well as the carbon nanofoams[17] support (b) showed both very similar initial performance, as well as similar performance after the degradation. Finally, the GNFs (c), as well as the VGFs (d), both showed a lower decrease in performance due to the degradation test compared to the conventional Vulcan carbon.

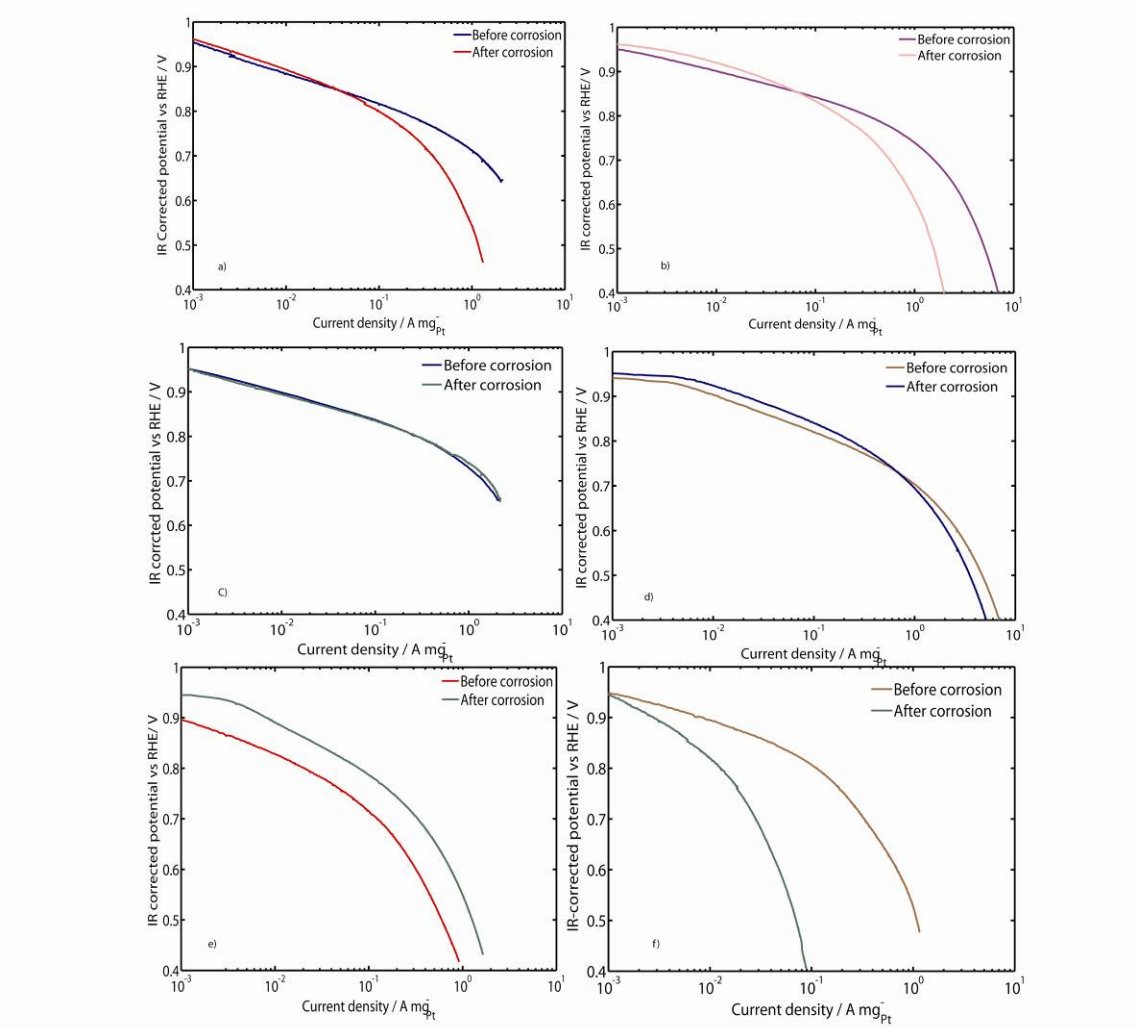

Figure 6.4. Polarization of cathodes before and after the degradation test. The polarization curves were recorded at 80 °C, fully humidified O_2 at the cathode and fully humidified H_2 at the anode.

It was found that the GNFs were highly corrosion resistant and therefore no observable degradation was seen. On the other hand, the VGF electrodes did suffer from some degradation as it was shown by both the cyclic voltammograms in Figure 6.3 (d) and polarization curves in Figure 6.4 (d). However, it was proposed that the performance loss at high current densities was not as severe as for the Pt/Vulcan electrode due to that the porous structure of the electrode did not collapse when corroded. Indeed, the SEM images in Figure 6.5 possibly support this theory, making these types of materials very attractive as materials for supporting the Pt catalyst in PEMFC electrodes.

[17] L.L Hussami, Carbon, 48 (2010) 3121

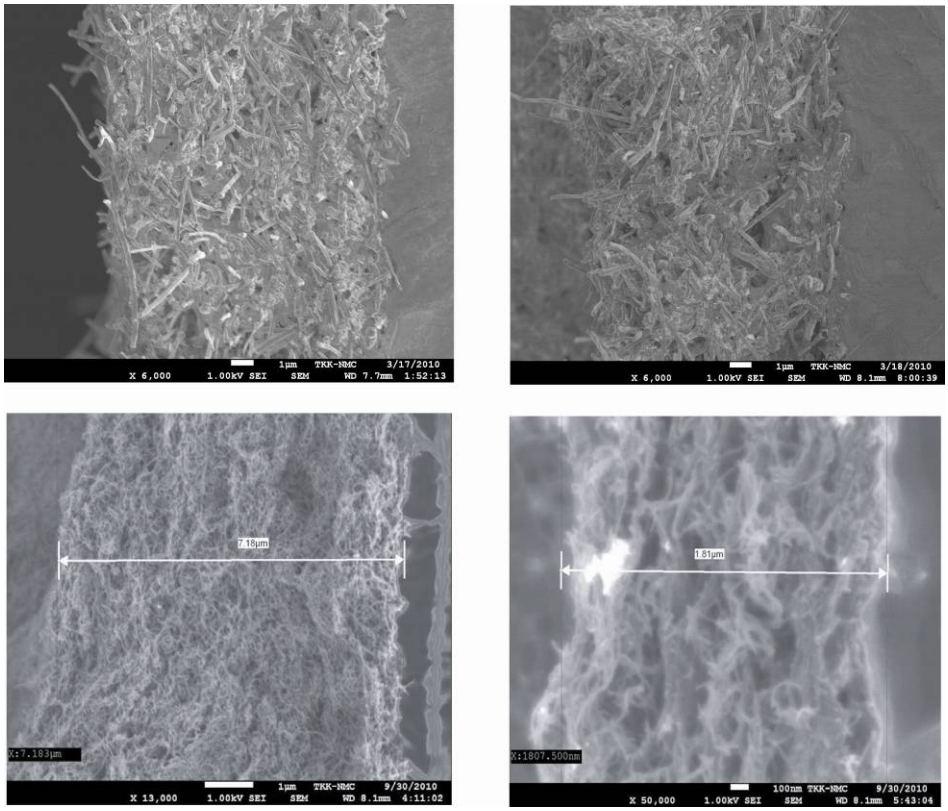

Figure 6.5. SEM-images Pt/GNF before (top left) and after degradation (top right) and Pt/VGF before (bottom left) and after (bottom right) degradation.

6.1.3 *In situ* Pt degradation studies

Some of the most interesting catalyst samples were tested for Pt dissolution in real PEM fuel cell conditions at KTH. The tests comprised of CVs and polarization curves for the determination of ECSA and fuel cell performance, respectively. The conditions for the CVs were: potential window 0.1-1.2 V vs. RHE, cycling speed 100 mV s^{-1}, 5 % H_2 in N_2 and N_2 as gases on anode and cathode respectively, the humidity of gases 100 % RH, and cell temperature 80 °C. The polarization curves were recorded in real fuel cell conditions: potential window 0.4 V-OCP vs. RHE, cycling speed 1 mV s^{-1}, 100 % RH H_2 and O_2 on anode and cathode respectively, cell temperature 80 °C. The results were compared to a catalyst supported on Vulcan.

The conditions of the actual degradation routine were 1.2-0.6 V vs. RHE, 80 °C, 100 % RH, O_2/H_2. Pt supported on Vulcan was again used as a reference. The potential was cycled for several thousands of cycles, after which the ECSA and performance of the samples were re-checked.

Table 6.1 shows the ECSA of the samples before and after Pt degradation routine. It can be seen that the ECSA of all Pt/GNF samples remained lower than that of BASF catalyst. An estimation of the real ECSA of the PANI treated samples (MP042-043) was impossible to give due to the very broad double layer charging area, which indicated that polyaniline residues capable of causing a high capacitive current in the sample were still present despite the pyrolysis step. The acid treatment of the support did not seem to increase the ECSA of the catalyst. The acid treated samples synthesized by the polyol method (TKK-GNF-001 and TKK-GNF-007) seemed to have a somewhat larger ECSA compared to acid treated samples prepared by the impregnation method.

Table 6.1. ECSA of the samples before and after the Pt degradation routine, as well as the decrease in ECSA proportioned to the number of the degradation cycles.

Sample	Initial ECSA ($cm^2\ mg_{Pt}^{-1}$)	ECSA after degradation ($cm^2\ mg_{Pt}^{-1}$)	No. of cycles	Decrease in ECSA ($cm^2\ mg_{Pt}^{-1}$ per 1 000 cycles)
MP023	21.3	6.6	8 500	1.73
MP034	15.0	n.a.	-	-
MP035	16.2	2.5	8 500	1.61
MP036	17.4	n.a.	-	-
TKK-GNF-001	45.7	n.a.	-	-
TKK-GNF-007	31.6	n.a.	-	-
MP042	indeterminable	indeterminable	300	-
MP043	indeterminable	indeterminable	300	-
BASF	117	23	7 200	13.1

* Samples consisting of GNFs acid treated at VTT, see Table 2.1, with Pt deposited by polyol method at Aalto University.

When the decrease in ECSA was proportioned to the number of degradation cycles, it could be noticed that the loss of electrochemically active surface area is the smallest in samples MP023 and MP035. However, the values of these samples were so close to each other that it could not be concluded that the acid treatment of the support would improve the catalyst stability. The greatest loss of ECSA occurred in BASF sample as presumed.

The most significant loss in fuel cell performance observed at 0.65 V occurred in PANI treated samples, see Table 6.2. Curiously, the current output at 0.65 V improves in samples MP023 and MP035 despite the loss of ECSA. It was suggested that the degradation routine caused changes in the electrode structure, e.g. deformation of the catalyst support led to improved contact between the fibers and Pt nanoparticles.

Table 6.2. Current densities at 0.65 V vs. RHE before and after the Pt degradation routine.

Sample	Initial current density (A mg_{Pt}^{-1}) at 0.65 V	Current density (A mg_{Pt}^{-1}) at 0.65 V after degradation
MP023	0.09	0.20
MP034	0.04	n.a.
MP035	0.06	0.08
MP036	0.11	n.a.
TKK-GNF-001	0.09	n.a.
TKK-GNF-007	0.09	n.a.
MP042	0.27	0.02
MP043	0.26	0.04
BASF	0.33	0.18

6.2 Experimental work at SDU

6.2.1 Thermal corrosion of carbon in Pt catalysts

Carbon thermal corrosion properties were examined at 200 °C. Samples were packed individually in aluminum foil of which weight was proven to be stable during the treatment. The weights of the small packages were examined via a digital balance. The samples were pre-heated at 80 °C to eliminate adsorption water. The weight loss corresponded to carbon corrosion, provided that the noble metal catalyst is thermally stable at 200 °C[18].

[18] Ma S., VDM Verlag (June 11,), ISBN-10: 363916704X, ISBN-13: 978-3639167047, 2009.

13 samples were tested as listed below in Table 6.3. The blank is empty aluminum foil as control. The weight losses were converted to carbon weight losses according to the information presented in the table.

Table 6.3. List of samples tested for thermal corrosion properties.

Name	Element content	Catalyst wt %	Alloy ration	Carbon type	Catalyst diameter nm according to XRD	Surface area m^2/g
GNF	C	0	-	CNF	-	13
GMWCNT	C	0	-	CNT	-	117
Vulcan	C	0	-	Vulcan	-	209
Ketjenblack	C	0	-	HSCB*	-	1421
Pt/GMWCNT	Pt/C	20	-	CNT	3.1	90
BASF	Pt/C	20	-	Vulcan	2.5	112
Hispec 9000	Pt/C	57.84	-	Vulcan	5.47	103
Hispec 9100	Pt/C	56.76	-	**	2.77	305
Hispec 10000	PtRu/C	59.72	1 to 1	Vulcan	2.9	114
Hispec 10100	PtRu/C	58.61	1 to 1	**	2.28	287
Pt/GNF	Pt/C	20	-	CNF	2.79	10
TEC 10EA	Pt/C	46.1	-	#	1.36	93
Blank	-	-		-	-	-

* High surface area carbon black
** Hispec 9100 and 10100 have the same type of carbon support, however the details are unknown.
# Special type of carbon, the details are unknown due to confidentiality.

All the carbon samples are illustrated in Figure 6.6. The blank sample was rather stable over the treatment period. All the carbon samples showed less than 1 % weight loss. This might be due to re-adsorption of trace of water or other gas molecules and organic substances. Within the first 10 hours, all samples reached a stable value. Based on the experimental data, no obvious difference was observed for carbon black (Vulcan) and CNT or CNF type carbon.

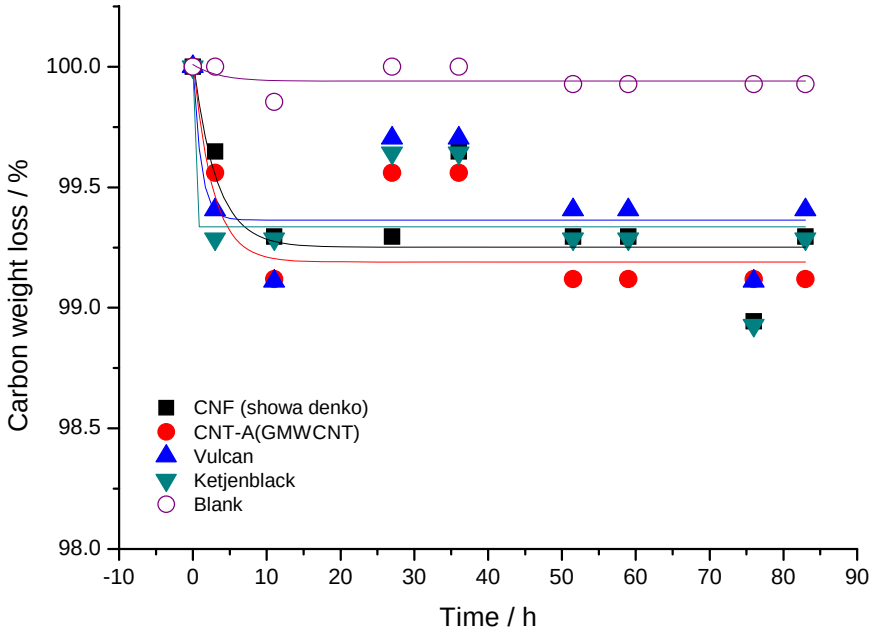

Figure 6.6. Carbon thermal decomposition in carbon samples.

CNT and CNF based catalysts were isolated and compared with Vulcan based catalyst in Figure 6.7. As shown in the result, for CNT (Pt/GMWCNT) and CNF (Pt/VGF) based catalyst, carbon degrades very similarly. Moreover, both of them are superior to Vulcan based catalyst (BASF). Comparing to the Japanese catalyst TEC 10EA,

Pt/GMWCNT and Pt/VGF demonstrate better thermal stability as well. However, the fast weight loss of TEC 10EA within the first 10 hours may also due to decomposition of organic substances.

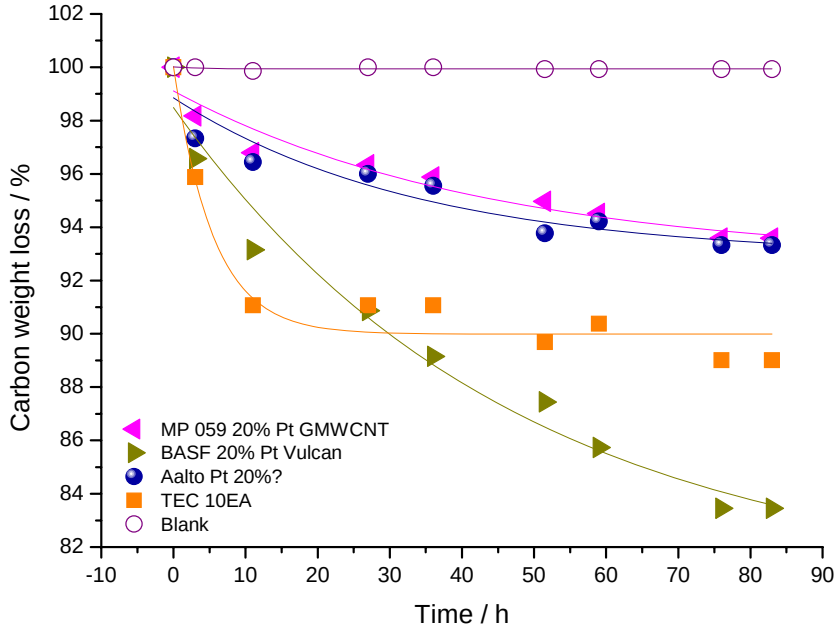

Figure 6.7. Carbon thermal decomposition in CNF and CNT based catalyst samples compared to Vulcan based catalyst (BASF).

Thermal behavior of Vulcan based catalysts was isolated and plotted in Figure 6.8. It clearly illustrates that the vulnerability of the supporting carbon was enhanced by increasing platinum loading and choice of catalyst alloy (BASF: 20 wt% Pt, Hispec 9000: 57.84 wt% Pt and Hispec 10000: 59.72 wt% PtRu).

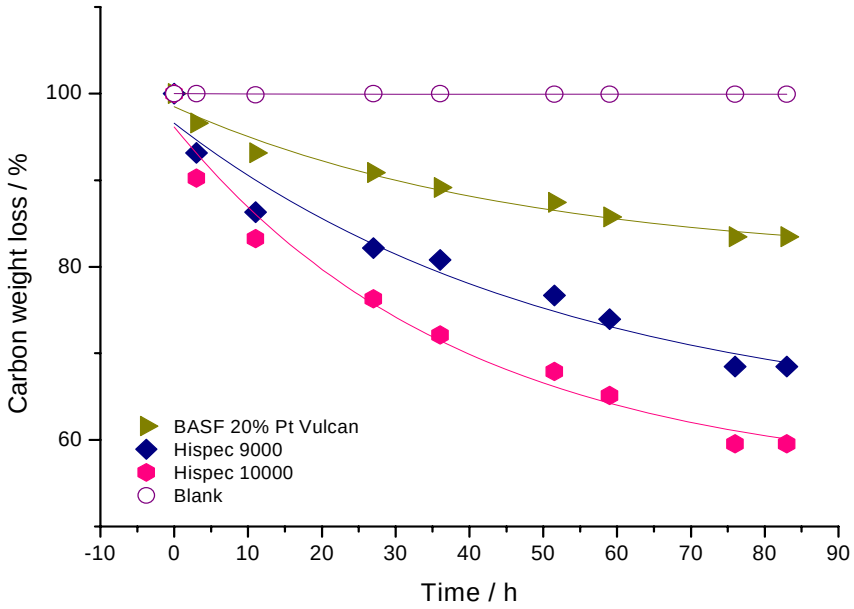

Figure 6.8. Carbon thermal decomposition from Vulcan based catalyst.

Johnson Matthey catalyst Hispec series were compared as shown in Figure 6.9. It shows that the carbon support in Hispec 9100 and 10100 is more thermally unstable than Vulcan type carbon.

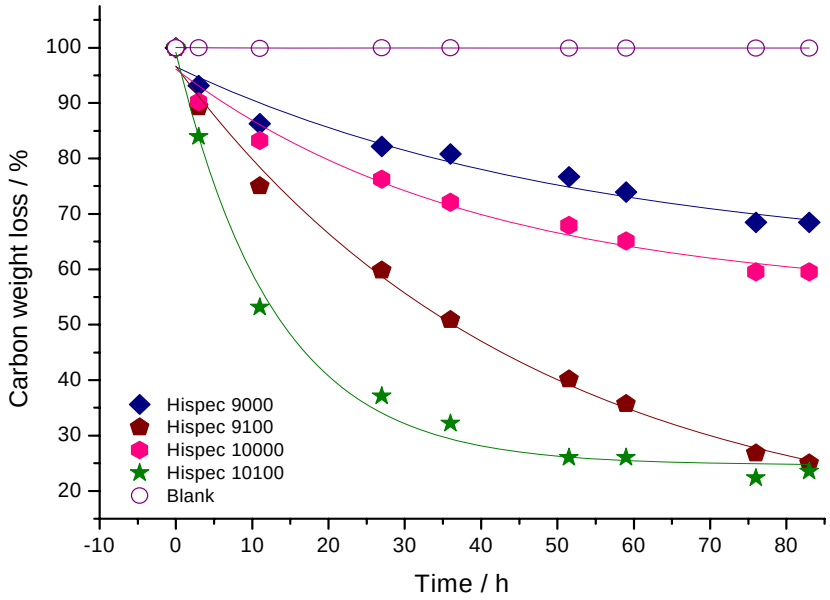

Figure 6.9. Carbon thermal decomposition in Johnson Matthey Hispec catalysts.

As a conclusion, GNF and GMWCNT demonstrated outstanding stability against carbon corrosion of less than 5 % compared to carbon black (Vulcan) support with 20 % carbon weight loss. Carbon corrosion was seen increasing with increasing platinum loading.

6.2.2 Carbon thermal decomposition in Pt catalyst

Suitable amounts of catalyst or carbon were weighted and mixed with Nafion ionomer solution. Thermogravimetric data, gathered by Setaram TG-DGA 92, of different carbon and catalyst samples are presented in Figure 6.10. As shown in the data, the normal thermal decomposition of carbon occurred around 645 °C (Vulcan). However under the catalytic influence of noble metal – platinum, the decomposition temperature of Vulcan decreased to around 400 °C (9000 + Nafion ionomer). CNTs and CNFs were influenced by the catalyst in a lesser degree, and the decomposition temperature was around 480 °C. In addition, Nafion ionomer, which is an important component in the PEM fuel cell, was also found to express better thermal stability when it was mixed with CNT or CNF based catalyst when compared to Vulcan based catalyst.

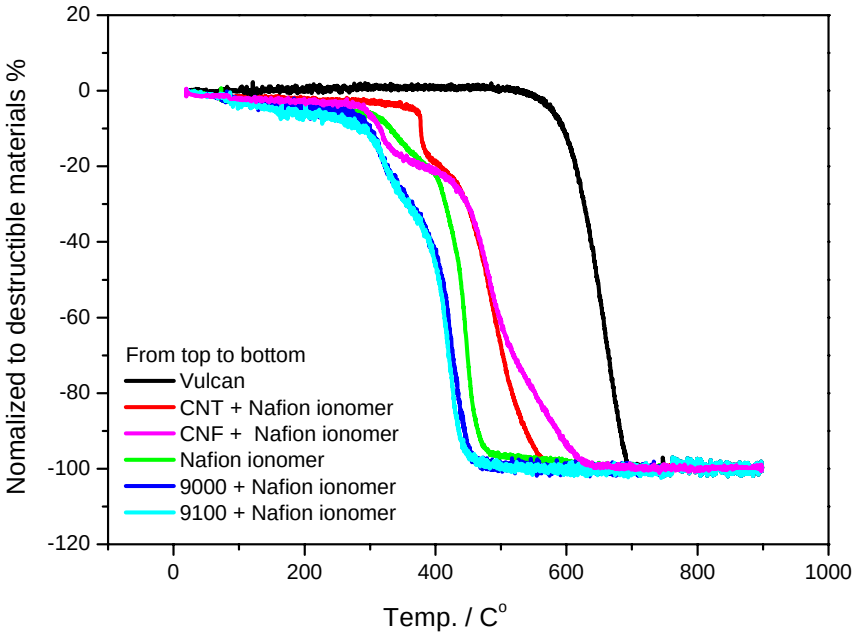

Figure 6.10. TG spectra of different carbon and carbon supported catalyst samples. Catalyst samples consist of approximately 20 wt% Pt on CNT, CNF or Vulcan (9000) support. Pure Nafion ionomer is included as well.

6.3 EQCM studies at SINTEF

In this study, an electrochemical quartz crystal microbalance (EQCM) instrument (Elchema EQCN-700) was used with 10 MHz EQCM crystals with electrodes made of gold and platinum. Experiments were performed on the electrodes prepared from commercial fuel cell catalyst (Alfa Aesar, nominally 50 wt % Pt on carbon, average particle size of 3.51 nm), in-house made platinum black material synthesized by reversed micro emulsion or with electrodeposited platinum from a hexachloroplatinic acid solution. All experiments were carried out in a deaerated 0.5 M H_2SO_4 solution at room temperature. A three-electrode setup with an Au wire counter electrode and a reversible hydrogen electrode (RHE) reference electrode was used.

Figure 6.11 shows CVs for Pt/C electrodes exposed to three different levels of chloride contamination and an additional experiment performed in pure sulfuric acid for reference. The data was normalized with respect to the Pt electrochemical active area. The presence of chloride in the electrolyte significantly shifted the platinum oxide formation to higher potentials, and the platinum surface appeared to be without a protective oxide film at voltages as high as 1.0 V when the chloride concentration was more than 20 ppm. A higher concentration of chloride did not seem to lead to a further increase in the oxidation onset potential beyond 1.0 V.

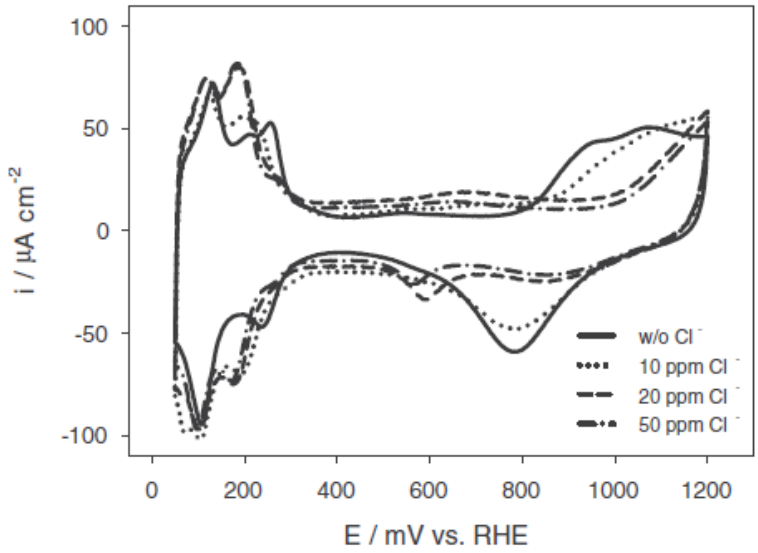

Figure 6.11. CVs for Pt/C electrodes exposed to three different levels of chloride contamination and an additional experiment performed in pure sulphuric acid for reference. The data was normalized with respect to the Pt electrochemical active area.

Figure 6.12 shows the mass change in Pt/C-based electrodes when kept at 1.2 V in 0.5 M H_2SO_4 with different levels of chloride in the solution. For all concentrations of chloride, except 50 ppm, all mass grams showed an initial increase in mass probably due to the formation of an initial platinum oxide layer on the electrode surface. After this initial increase in mass, the electrodes exposed to the electrolyte containing chloride started to decrease in mass. The rate of mass loss increased with increasing concentration of chloride in the electrolyte. The mass loss curves for the electrodes exposed to a chloride-containing electrolyte showed a linear trend, indicating a constant degradation rate subsequent to the initial period where an oxide layer was still being formed.

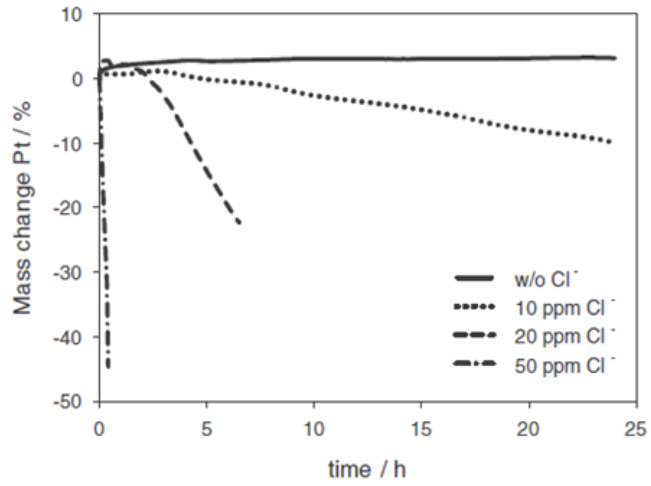

Figure 6.12. Mass change in Pt/C-based electrodes when kept at 1.2 V in 0.5 M H_2SO_4 with different levels of chloride in the solution.

It was found that platinum metal surfaces based on particles and films showed a large difference toward dissolution when exposed to small amounts of chloride. While a platinum metal film showed no degradation in a sulfuric acid solution containing 10 ppm of chloride, an electrode made from platinum nanoparticles supported on carbon lost 10 % of its platinum content over a 24 h period when exposed to the same amount of chloride.

The observed platinum dissolution for the Pt/C catalyst material was highly dependent on the amount of chloride that was introduced to the electrolyte solution. A fivefold increase in the concentration of chloride (from 10 to 50 ppm) resulted in an observed dissolution rate that was approximately 170 times larger.

The EQCM proved to be a useful technique to assess the durability of fuel cell catalyst materials. The high resolution and continuous capabilities of the EQCM make it useful for observing degradation processes. In combination with additional techniques such as CV, one can distinguish between performance loss caused by particle agglomeration and growth, and degradation related to loss of platinum metal from the catalyst by dissolution.

7 MEA degradation studies

7.1 Experimental work at SDU

7.1.1 Electrochemical stability in acidic aqueous media

For catalyst support inside the membrane electrode assembly (MEA) of the PEMFC, electrochemical stability is even more important requirement for good performance of the cell than thermal durability. Therefore, electrochemical stability of the carbon support, based on platinum dissolution in acidic media was conducted via cyclic voltammetry. Detection of platinum dissolution was conducted by atomic absorption spectroscopy (AAS)[19].

A home-developed Teflon cell was used for MEA catalyst degradation studies as shown in Figure 7.1. The liquid electrolyte was 1 M sulfuric acid. Standard high loading Pt and PtRu electrodes and low loading PtRu/C (IRD) electrode was studied in this work. Normally a MEA with one electrode is enough to conduct the experiment. The MEA was sandwiched between two Teflon blocks. The counter electrode was clean carbon paper gas diffusion layer (GDL) with no extra additives. For dissolution studies, the potential sweep rate was kept constant 0.1 V/s; a liquid sample was taken by a syringe at each potential step after 30 minutes potential cycling. An atomic adsorption spectrometer (Perkin-Elmer 2380) with graphite oven (Perkin-Elmer HGA-300 Programmer) was used for noble metal detection in liquid solutions.

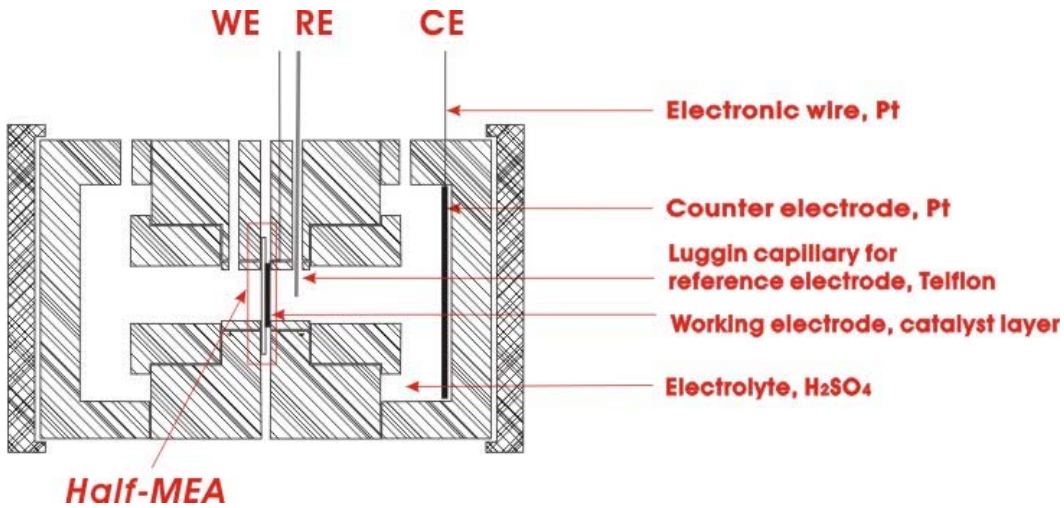

Figure 7.1. Setup for testing the electrochemical stability of the MEAs.

In order to make a reasonable comparison, catalysts with proximate properties were chosen for the measurement. Catalysts BASF and TKK are both with 20 wt% platinum loading, but in BASF Pt is supported on Vulcan and in TKK on CNFs, respectively. The results of the dissolution tests are shown in Figure 7.2.

[19] S. M. Andersen et al., Solid State Ionics, internet available, 2010.

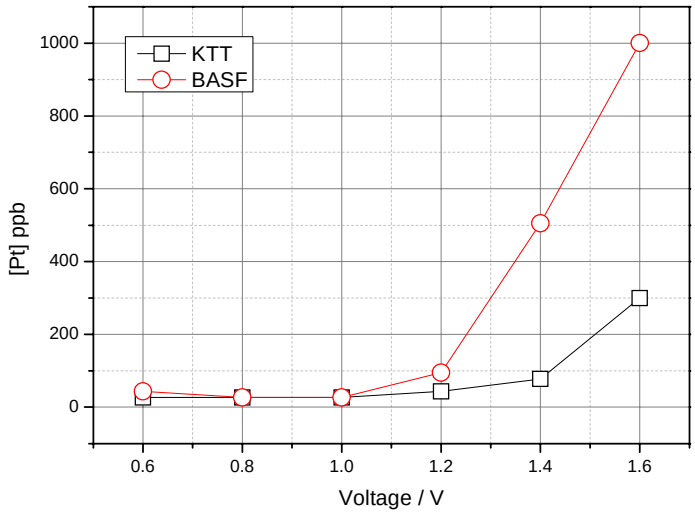

Figure 7.2. Dissolution of Pt on Vulcan (BASF) and CNFs (TKK) in acidic media.

It can be seen that at potential lower than 1.0 V vs. RHE, the two catalysts had very similar dissolution properties. This might be due to the similar properties of the noble metal. However, at higher potential, CNF supported catalyst (TKK) showed about 4 times less dissolution compared to BASF catalyst supported on Vulcan. As it is well known, platinum dissolution at higher potential is mainly due to electrochemical corrosion of carbon support[20].

7.1.2 Electrochemical stability under high voltage cyclic treatment

Full MEAs with commercially available Johnson Matthey as the anode and various carbon supported Pt catalysts as cathode were tested for electrochemical stability in a single cell. All MEAs were prepared by IRD fuel cells. Anode was purged with hydrogen and cathode with nitrogen. In this way anode functioned as counter and reference electrode and cathode as working electrode, respectively. The cathode catalyst was kept under high voltage (up to 1.6 V) cycling treatment. The potential was cycled for 5 000 times and then another 10 000 times. The ECSA of the cathode catalyst and the maximum power density of the single cell were determined before and after each treatment. The results are summarized in Table 7.1.

Table 7.1. Results of the electrode electrochemical stability tests under high potential cycling.

		Loading (mg/cm^2)	ECSA (cm^2/mg)	ECSA change (%)	Max power density (W/cm^2)	Max power density change (%)
BASF (Vulcan)	**Fresh**	0.518	779	-	0.393	-
	After 5k	0.518	463	-41	0.315	-20
	After 10k	0.518	392	-50	0.306	-22
VGF	**Fresh**	0.529	331	-	0.195	-
	After 5k	0.529	426	+29	0.276	+42
	After 10k	0.529	330	0	0.218	+12
MWCNT	**Fresh**	0.530	310	-	0.147	-
	After 5k	0.530	328	+6	0.176	+20
	After 10k	0.530	248	-20	0.156	+6

[20] Avasarala B. et al. Electrochemica ACTA55(16), 4765-4771, 2010.

As shown in the results, carbon nanofiber and nanotube based catalysts showed better stability under the high voltage cyclic treatment. Vulcan based platinum lost 40 % of the active surface area after 5000 cycles, whereas both VGFs and MWCNTs showed higher active area and better single cell performance, which might due to an activation process or electrode structure reorganization. For a long perspective, CNTs and CNFs are more valuable than carbon black owing to their outstanding durability in fuel cell conditions.

7.1.3 Single cell testing

MEA sample preparation was provided by IRD. Sample details are summarized in Table 7.2.

Table 7.2. List of MEA samples prepared at IRD for single cell testing.

Group	Details	Catalyst, Ionomer, and procedure
1	Full MEA: JM|BASF Half MEA: anode: JM, cathode: BASF, JM, TKK	Anode Hispec 9000 30 wt% ionomer Chemical deposition
2	Full MEA: JM|BASF, JM|JM, JM|TKK Half MEA: anode: JM, cathode: BASF, JM, TKK	Anode Hispec 9000 40 wt% ionomer Chemical deposition
3	Half MEA: cathode of different deposition sweep	30 and 0 % ionomer Sputtering
4	Full MEA: JM|BASF, JM|MWCNT, JM|AALTO Half MEA: BASF, MWCNT, AALTO	Anode Hispec 9100 40 and 50% ionomer Chemical deposition

Setup for single cell test at SDU is shown in Figure 7.3. Gas flow controllers supplied H_2 and air. Gas temperature was regulated with water and cell temperature was controlled by heat elements. The maximum operation temperature was limited to 70 °C. Electrochemical workstation (Zahner IMe6) was used for current control and monitoring of potential change. Electrochemical impedance measurements were also performed by the instrument.

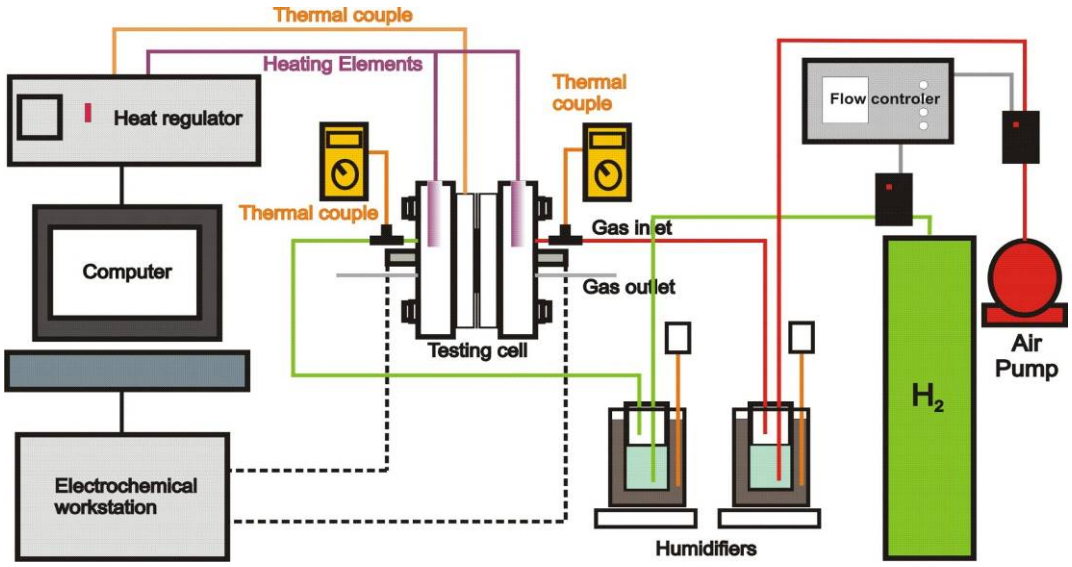

Figure 7.3. Single cell experimental setup

Major components of the single cell are shown in Figure 7.4. In the experiment, MEA was sandwiched between the two graphite plates. For an easy startup, anode was designed the same as cathode.

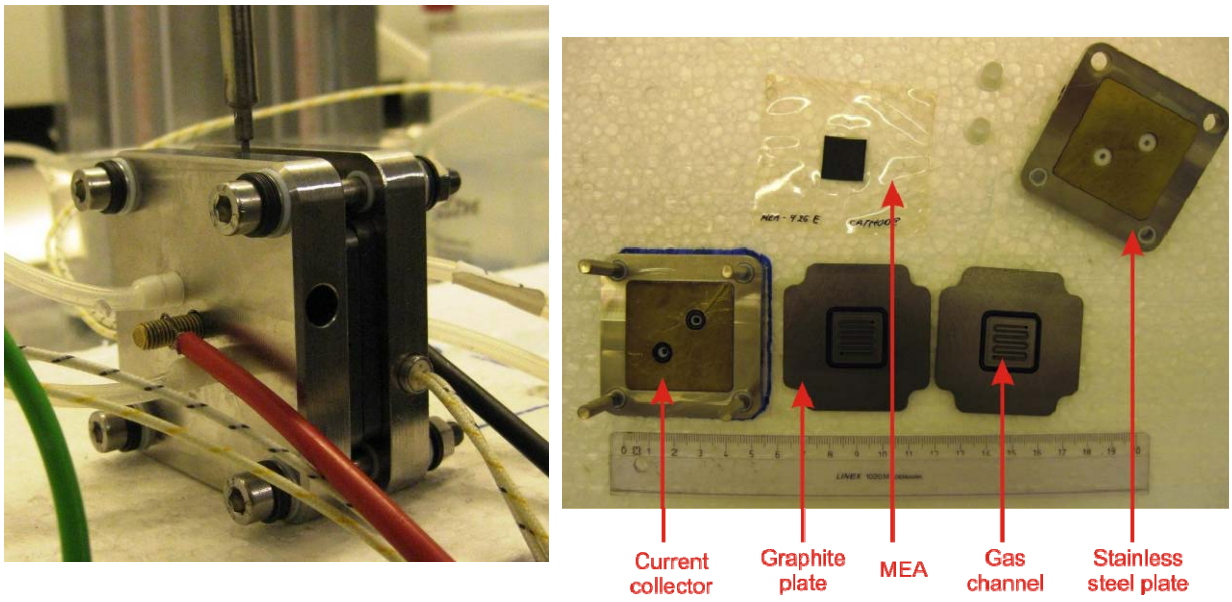

Figure 7.4. Major components of the single cell setup.

Carbon nanofiber based platinum catalyst demonstrated a lower single cell performance at 80 or 70 °C, 100% humidity (H_2 0.2 mL/s and air 1.0 mL/s) comparing to carbon black based Pt catalyst. This might be due to the design of the MEA based on traditional carbon black supported catalyst; the cell performance could be optimized via varying the MEA components and tuning the content. 40% Nafion ionomer content was found best performance among samples of 0, 30, 40 and 50% ionomer loading. The polarization curves and impedance measurement results of the MEA group 4 are showed as an example in Figure 7.5.

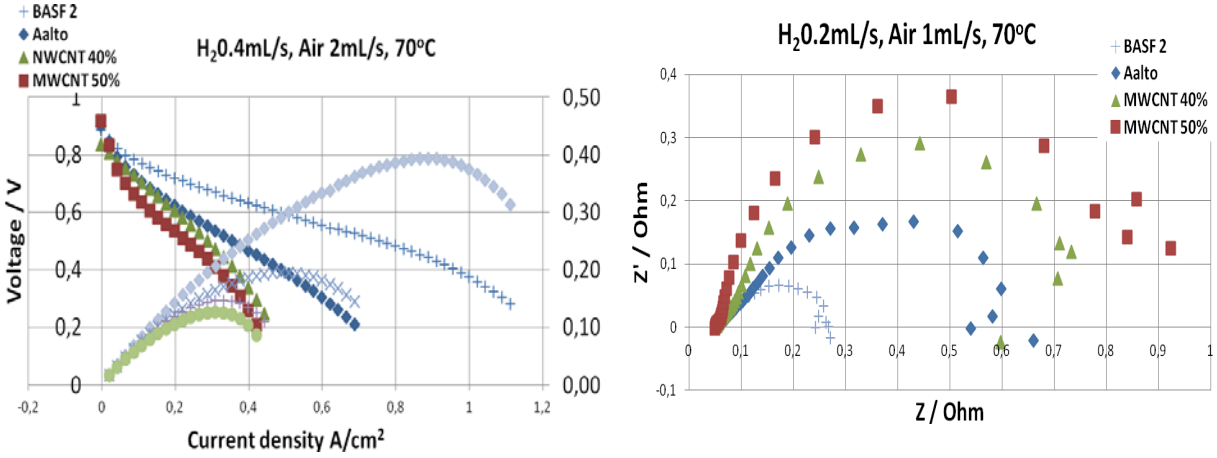

Figure 7.5. Polarization curves and impedance results of the group 4 MEA samples.

7.2 Experimental work at SINTEF

7.2.1 *In situ* carbon corrosion measurements

MEAs for accelerated *in situ* carbon corrosion tests were manufactured by IRD Fuel Cells by screen printing method. The Pt catalysts used in these 3 cm^2 MEAs were synthesized by the polyol method on acid treated GNFs. The MEAs comprised of a commercial catalyst (Johnson Matthey, 20 wt% Pt on Vulcan XC-72) on the anode side and a Pt/GNF catalyst, or a reference catalyst (BASF, 20 wt% Pt on Vulcan XC-72), on the cathode side. The catalyst loading on the anode and cathode was 0.3 mg cm^{-2} and 0.5 mg cm^{-2} respectively.

Accelerated *in situ* carbon corrosion tests were performed in order to compare the durability of GNF and Vulcan based catalysts. The MEAs were mounted in a Fuel Cell Technologies test cell with serpentine carbon flow fields and connected to an automated test station with Fuel Cell Technologies membrane humidifiers. Before starting

the carbon corrosion protocol, the MEAs were activated by running the cell at 0.7 V and 0.25 V with 10 minutes intervals at 70°C, 100 % RH and a stoichiometry of 1.2 and 2.5 on the anode and cathode respectively. The activation procedure was ended when no additional improvement in performance could be observed.

The measurement procedure consisted of carbon degradation routine (0.6-1.5 V vs. RHE, 40 mV/s, air/H_2, 70 °C, 100 % RH, 300 cycles) simulating the elevated voltages occurring at start up/shut down cycles of the cell. The cathode exhaust gas was analyzed for CO_2, CO, SO_2, CHOH, CHOOH, and HF using a Gasmet CR4000 FTIR gas spectrometer connected to the cathode outlet port of the test cell by a heated 2-micron filter and gas line.

Figure 7.6 and Figure 7.7 present the results in the case of both CB and GNF based catalysts. It can be seen by the polarization curves in Figure 7.6 that the GNF supported catalyst was practically stable during the cycling conditions while the MEA based on the CB catalyst had experienced a detrimental degradation during the potential cycling. Moreover, the FTIR results in Figure 7.7 show that the amount of CO_2 in the cathode exhaust gas from the CB based MEA was significantly higher than that for the MEA based on the GNF catalyst. By integration of the CO_2 concentration curve, the amount of carbon lost by the catalyst was found to be 0.05 mmol for the CB catalyst and 0.01 mmol for the GNF catalyst, amounting to about 10 wt% and 2 wt% of the available carbon respectively. However, the measured CO_2 concentration in the exhaust gas of the VGCF based MEA was in the lower range of the detectable limit of the FTIR analyzer, thus the reported carbon loss for this catalyst was probably an overestimation of the real loss of GNF support material. These measurements verify that carbon nanofibers are a good choice as catalyst supports in PEM fuel cells, showing a carbon loss of less than 20 % compared to carbon black.

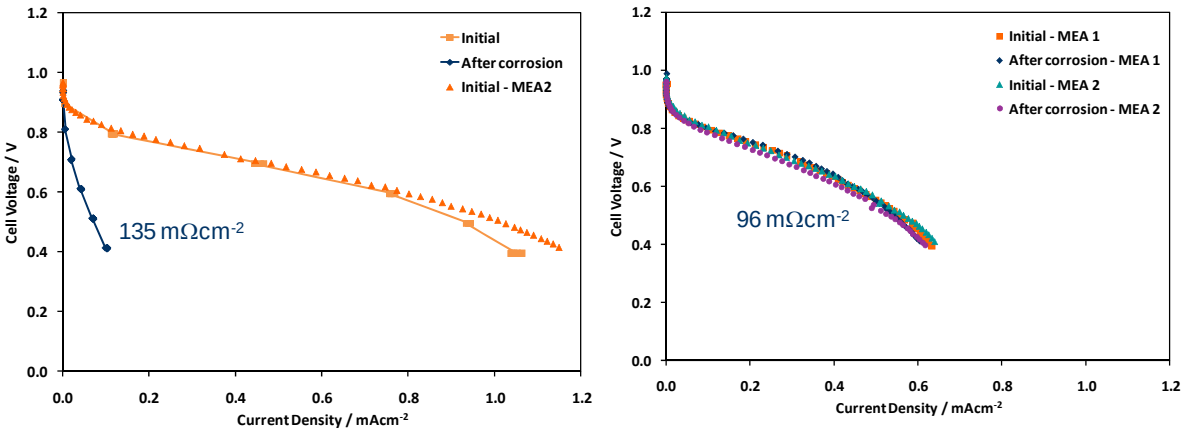

Figure 7.6 Polarization curves taken before and after carbon corrosion protocol. Left: Vulcan catalyst support, Right: GNF catalyst support.

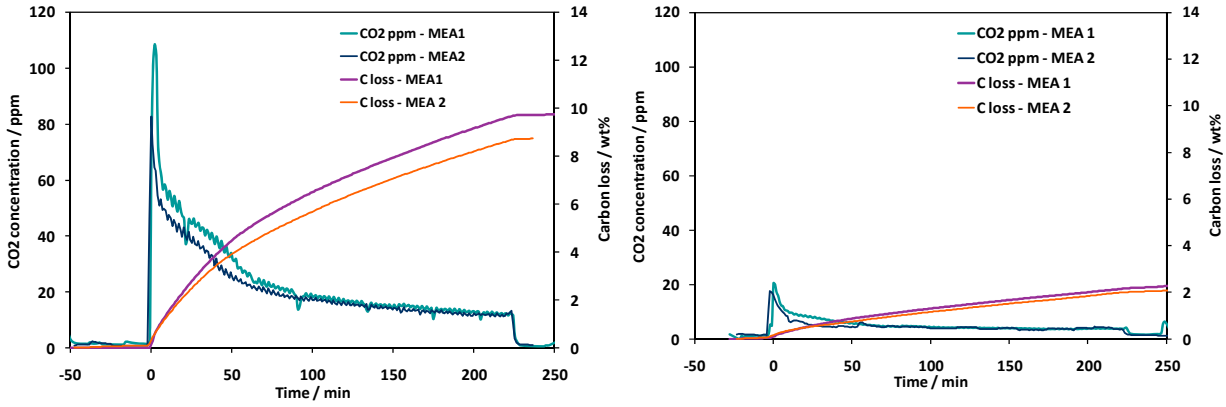

Figure 7.7. CO_2 concentration in cathode exhaust gas and the corresponding accumulated carbon loss from the catalyst support. Vulcan (left) and GNF (right).

7.2.2 Start-stop measurements

In addition to accelerated carbon corrosion tests, actual start-stop measurements of fuel cells were also performed. The same type of MEAs used for the *in situ* carbon corrosion measurements during accelerated carbon corrosion protocol described above was used. The fuel cell operated at open circuit at the start-up conditions when humidified hydrogen when supplied to the anode. At shut down, dry air was purged to the anode and the gas flows were not stopped during the shut-down period. Each purge interval was 15 minutes and the total duration of the protocol was 20 hours. Figure 7.8 schematically illustrates the start-stop procedure.

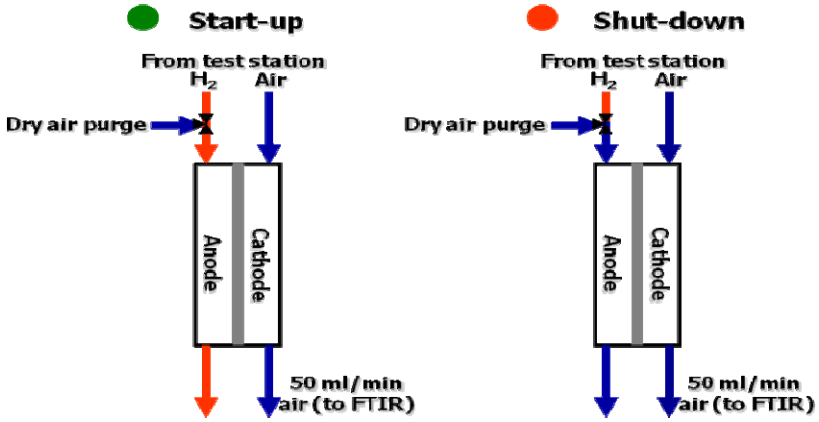

Figure 7.8 Procedure for start-stop measurements of the fuel cell.

Figure 7.9 shows polarization curves of the MEAs before and after the start-stop protocol. It can be observed that the fuel cell based on the GNF support increased its performance while the corresponding MEA based on CB supports degraded, showing significantly lower performances in the low current range. Cathode exhaust gas CO_2 emissions measured by FTIR (Figure 7.10) further explains this by showing larger CO_2 emissions from the CB based fuel cell, confirming that the GNF has a higher stability towards start-stop cycling than CB.

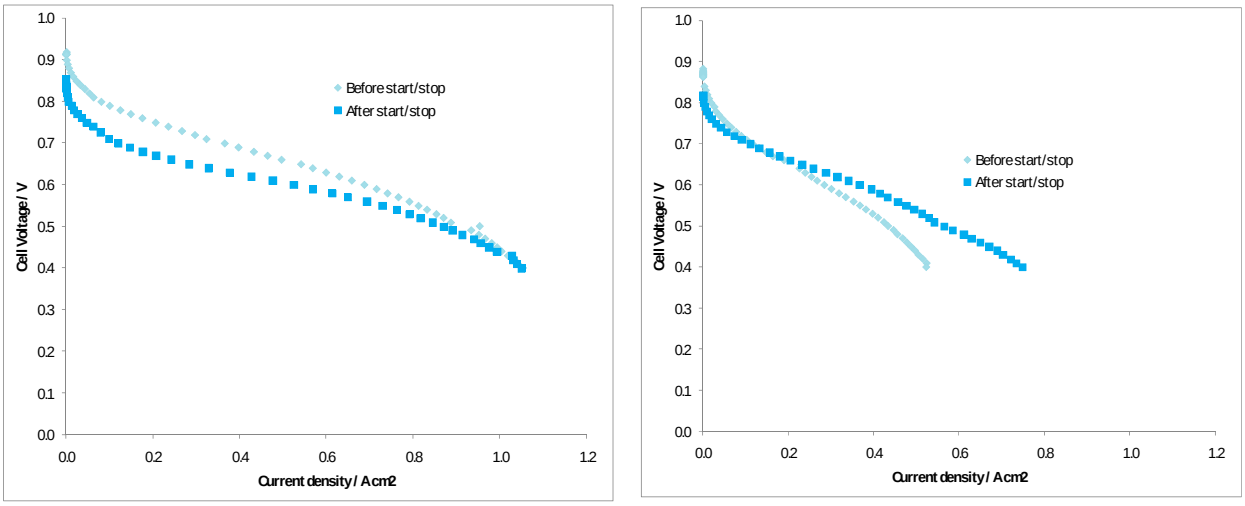

Figure 7.9. Polarization curves recorded before and after the start-stop protocol. Left: CB catalyst support, Right: GNF catalyst support.

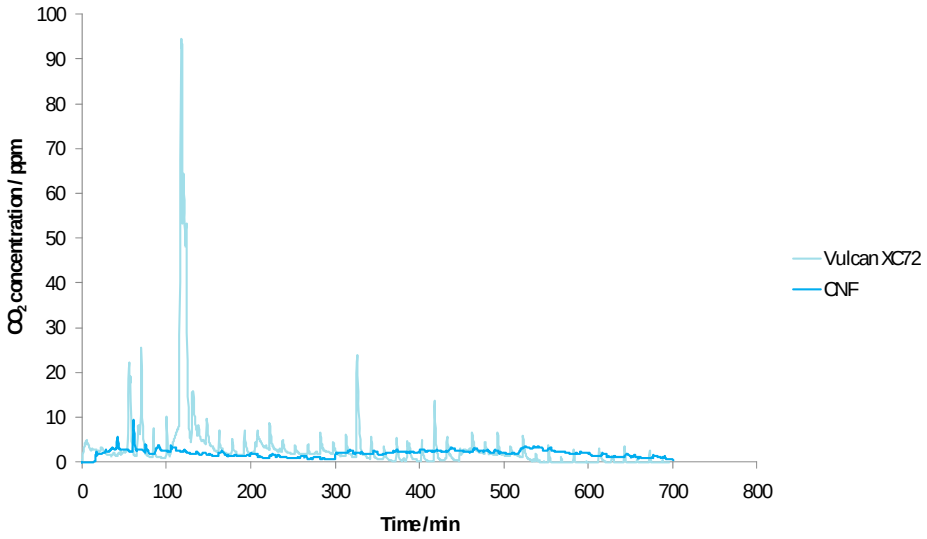

Figure 7.10. CO_2 concentration in cathode exhaust gas for PEM fuel cell. Vulcan XC-72 is the used carbon black support, whereas CNF refers to GNF.